NAVAL POSTGRADUATE SCHOOL

Monterey, California

THESIS

VELOCITY COMPENSATION IN STEPPED FREQUENCY RADAR

by

Yu-Bin Ma

December 1995

Thesis Advisor: Gurnam S. Gill

Second Reader: David C. Jenn

Approved for public release; distribution is unlimited.

Approved for public release; distribution is unlimited.

VELOCITY COMPENSATION IN STEPPED FREQUENCY RADAR

Yu-Bin Ma
MAJ., R.O.C Army
B.S.E.E., Chung Cheng Institute of Technology, 1987

Submitted in partial fulfillment
of the requirements for the degree of

MASTER OF SCIENCE IN ELECTRICAL ENGINEERING

from the

NAVAL POSTGRADUATE SCHOOL
December, 1995

Author: Yu Bin Ma
Yu-Bin Ma

Approved By: L. S. Gill
Gurnam S. Gill, Thesis Advisor

David C. Jenn
David C. Jenn, Second Reader

Charles W. Therrien
Herschel H. Loomis Jr., Chairman
Department of Electrical and Computer Engineering

ABSTRACT

As compared to the commonly used constant frequency radar waveforms, the stepped-frequency waveform can achieve high range resolution while still retaining the advantages of lower instantaneous receiver bandwidth and lower analog-to-digital sampling rate. However, the relative radial motion between the target and the stepped-frequency radar will result in performance degradations, such as range error, loss in signal-to-noise ratio, and degraded range resolution. The solution to this problem is to apply velocity compensation to the received signal, which can eliminate the degradations due to Doppler effects. Three velocity compensation schemes for the detection of a moving target in clutter are designed, discussed, and compared in this thesis. Also, a simulation is presented to verify the concepts, and simulation results are compared and discussed.

(This page is intentionally left blank.)

TABLE OF CONTENTS

I. INTRODUCTION 1

II. PRINCIPLES OF THE STEPPED FREQUENCY RADAR 3

A. STEPPED FREQUENCY WAVEFORM 3

B. STEPPED FREQUENCY RADAR SYSTEM 5

C. HIGH RESOLUTION PROCESSING 10
1. Generation of HRR Profile 12
2 Maximum Unambiguous Range Window, R_u 14

D. EFFECTS OF THE RELATIVE RADIAL VELOCITY 15

E. SELECTION OF PULSE WIDTH, τ AND FREQUENCY STEP SIZE, Δf 18

III. VELOCITY COMPENSATION IN THE STEPPED FREQUENCY RADAR 23

A. VELOCITY COMPENSATION SCHEME 1 24

B. VELOCITY COMPENSATION SCHEME 2 25

C. ANALYSIS AND COMPARISON OF SCHEME 1 AND SCHEME 2 28

D. VELOCITY COMPENSATION SCHEME 3 30

E. SIMULATION 32
1. Effects of the Relative Radial Velocity 35
2. Simulation of Scheme 1 and Scheme 2 38
3. Simulation of Scheme 3 46

IV. CONCLUSION 53

APPENDIX A. SIGNAL MODELING 55

APPENDIX B. SIMULATION PROGRAMS IN MATLAB 59

LIST OF REFERENCES 69

INITIAL DISTRIBUTION LIST 71

I. INTRODUCTION

The stepped-frequency waveform is an interpulse version of pulse compression techniques in high resolution radars. In the stepped-frequency waveform, the carrier frequencies for a burst of N transmitted pulses are monotonically increased from pulse to pulse by a fixed frequency increment. The stepped-frequency radar can achieve high range resolution with the advantages of lower instantaneous receiver bandwidth and lower analog-to-digital (A/D) sampling rate, both of which are the major limiting factors for achieving high range resolution in the conventional constant frequency radar. The high range resolution of the stepped-frequency radar is obtained by coherently processing a series of N returns from the stepped-frequency pulses. The coherent processing is performed by taking the Discrete Fourier Transform (DFT) of N pulse returns, which acts as a matched filter when there is no relative radial motion between the radar and the target. The relative radial motion during the coherent processing interval will result in nonlinear phase shifts in the received signal. As a result, the DFT processing is not matched to the received signal, leading to a distorted range profile. The solution to this problem is to apply velocity compensation to the received signal based on the target velocity. This thesis mainly focuses on the study of velocity compensation in the stepped-frequency radar. The problem of the detection of a moving target in clutter will be discussed, which requires clutter cancellation to eliminate the clutter and velocity compensation to restore the target resolution.

Three velocity compensation schemes are designed and discussed in this thesis. In the first scheme, the velocity compensation is performed by multiplying by a compensation factor in the time domain, while in the second scheme, the velocity compensation is performed by circular convolution with the DFT form of the compensation factor in the frequency domain. Both schemes are conceptually equivalent, but have different implementations. Their implementations will be analyzed and compared. In the first and the second schemes, the target velocity is assumed to be known in advance. The third scheme is developed based on the first scheme with the addition of a velocity compensation loop which enables the target with unknown velocity to be processed; however, the target velocity is assumed within a defined interval. In addition, a computer simulation is presented to evaluate the detection of a moving target in clutter using the stepped-frequency waveform by means of the three velocity compensation schemes. The simulation results are discussed and compared.

In Chapter II, the principle of the stepped-frequency waveform and its corresponding radar system are introduced. The discussion of high range resolution processing and the analysis of related radar parameters are also included. In Chapter III, three velocity compensation schemes for the detection of a moving target in clutter are investigated. The simulation results of the three compensation schemes are also presented in this chapter. Conclusions from the work are provided in Chapter IV. The signal modeling and the computer programs used in the simulation are shown in Appendices A and B.

II. PRINCIPLES OF THE STEPPED FREQUENCY RADAR

A. STEPPED FREQUENCY WAVEFORM

The stepped-frequency radar transmits a burst of N pulses, whose carrier frequencies are monotonically increased from pulse to pulse by a fixed frequency step size, Δf as described in Figure 2.1. Each pulse has the same pulse width, τ, and is transmitted at a fixed pulse repetition frequency (PRF). The carrier frequency of the nth transmitted pulse is given by

$$f_n = f_0 + (n\text{-}1)\Delta f \tag{2.1}$$

where

f_0 = nominal carrier frequency

Δf = frequency step size

n = 1, 2, ..., N

The frequency spectrum constituted by a series of N returns from a target due to the stepped-frequency waveform is shown in Figure 2.2. Thus, the total effective bandwidth of the stepped-frequency waveform is given by

$$B_{eff} = N\Delta f \tag{2.2}$$

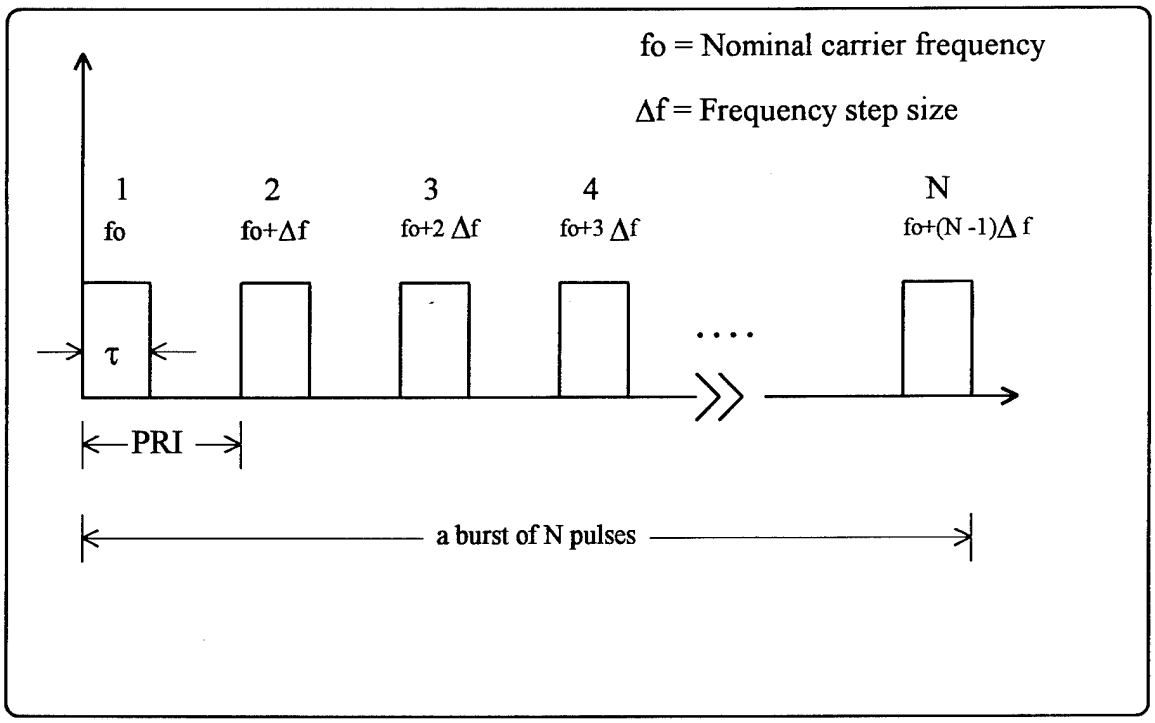

Figure 2.1 The Stepped-FrequencyWaveform.

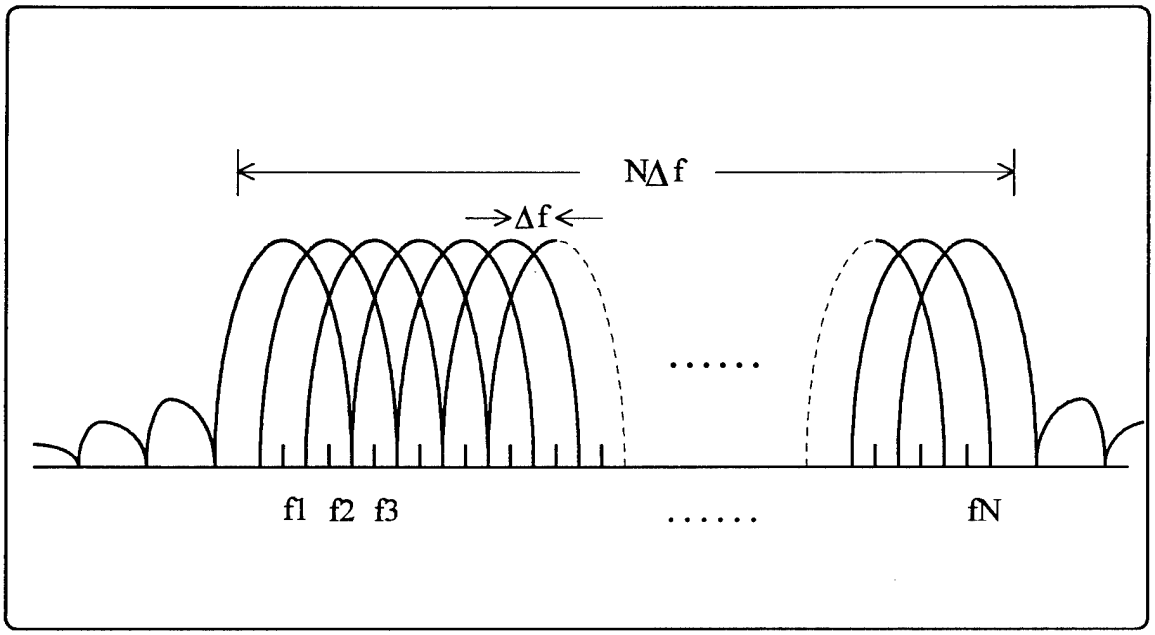

Figure 2.2 Total Effective Bandwidth of the Stepped-Frequency Waveform.

The 3-dB instantaneous bandwith of the stepped-frequency waveform is approximately equal to the inverse of the pulse width, $1/\tau$, and is much less than the total effective bandwidth of the waveform. It is noted that the range resolution of the stepped-frequency waveform radar is not the conventional range resolution, $c\tau/2$. The synthetic range resolution achieved by coherently processing a series of N returns from a target depends upon the total effective bandwidth and is given as

$$\Delta r = \frac{c}{2B_{eff}} = \frac{c}{2N\Delta f} \tag{2.3}$$

where

c = the speed of light, 3×10^8 m/sec

The synthetic range resolution, Δr, given by Eq.2.3 for a specific target can be improved either by increasing the number of transmitted pulses in a burst, N, or by increasing the frequency step size, Δf.

B. STEPPED FREQUENCY RADAR SYSTEM

The implementation of the stepped-frequency radar is similar to that of a coherent pulsed-Doppler radar. A block diagram of a stepped-frequency radar system is shown in Figure 2.3. The major changes in the stepped-frequency radar are the addition of a fast coherent stepped-frequency synthesizer, up-conversion and down-conversion circuitry, and the requirement for a wideband front end [Ref.2: p.236]. The core of the system is a coherent stepped-frequency synthesizer with the output frequency of f_{syn}. The frequency

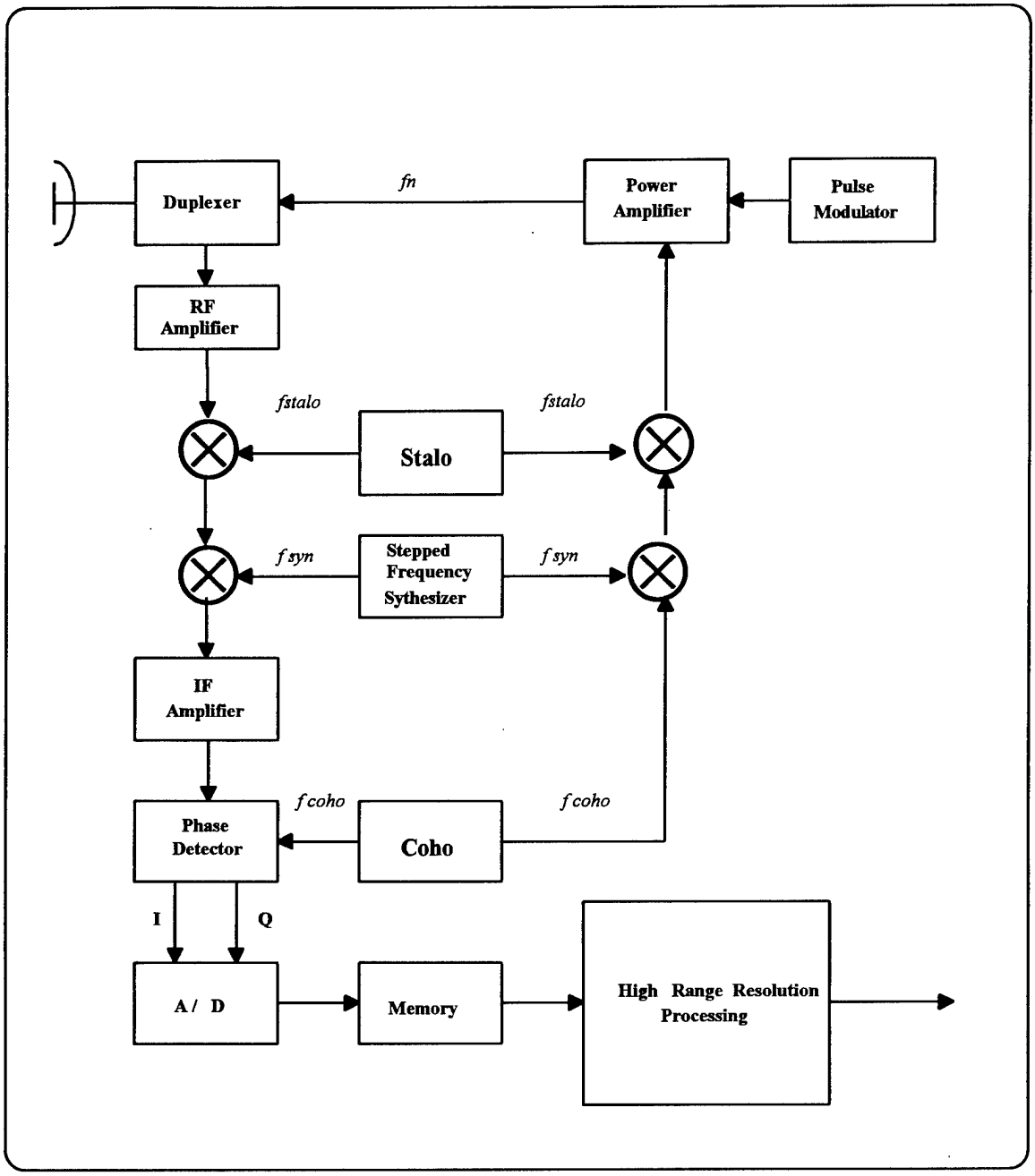

Figure 2.3 A Block Diagram of the Stepped-Frequency Radar.

of the synthesizer is stepped from pulse to pulse by a fixed frequency step size, Δf, and is written as

$$f_{syn} = (n\text{-}1)\Delta f \tag{2.4}$$

The stepped-frequency waveform is generated by first mixing the frequency of a coherent oscillator, f_{coho}, with the output frequency of the stepped-frequency synthesizer, f_{syn}. Following this up-conversion, the signal is converted to the final transmitted frequency by mixing with the frequency of a stable local oscillator, f_{stalo}. The sum frequency signal is then pulse modulated and amplified. Thus, the carrier frequency of each transmitted pulse is composed of three elements: the frequency of the coherent oscillator, f_{coho}, the frequency of the stable oscillator, f_{stalo}, and the variable stepped frequency, f_{syn} from the stepped-frequency synthesizer. The carrier frequency of the nth transmitted pulse can be written as

$$f_n = f_{stalo} + f_{coho} + f_{syn} = f_0 + (n\text{-}1)\Delta f \tag{2.5}$$

where

$$f_0 = f_{stalo} + f_{coho} = \text{ nominal carrier frequency}$$

On the receiver side, the return signal is first mixed with the fixed frequency of the stable local oscillator, f_{stal}, and then further down-converted by mixing with a sample of the stepped-frequency synthesizer. The output signal after the second mixer is the

intermediate-frequency (IF) signal which is then passed through an IF amplifier. The 3-dB bandwidth of the IF amplifier is approximately equal to the inverse of the pulse width, $1/\tau$, and is centered on the frequency of the coherent oscillator, f_{coho}. The stepped-frequency synthesizer is synchronized with the transmitter so that the transmitted carrier frequency and the output of stepped-frequency synthesizer use the same stepped frequency, f_{syn} within a pulse repetition interval (PRI). As a result, multiple-time-around target echoes after going through the second mixer will have frequencies varying by multiples of the frequency step size. Therefore, the target echo whose IF signal falls outside the passband of the IF amplifier (i.e., target echoes from different transmitted pulses with different f_{syn}) will be filtered out. The amplified signal is then split into two channels, the in-phase channel, I, and the quadrature channel, Q, which are mixed with the frequency of the coherent oscillator, f_{coho} in the phase detector. The in-phase signal is mixed with f_{coho} directly, and the quadrature signal is mixed with 90° shifted f_{coho}. The outputs of the phase detector are sampled and quantized in the A/D converter. It should be noted that typically, the sampling interval is τ seconds and thus each sample forms a range cell. The samples from the A/D converter are stored in memory and sorted by range cells. The collected N samples from a range cell in which the target is located will be used for high resolution processing as described in Figure 2.4.

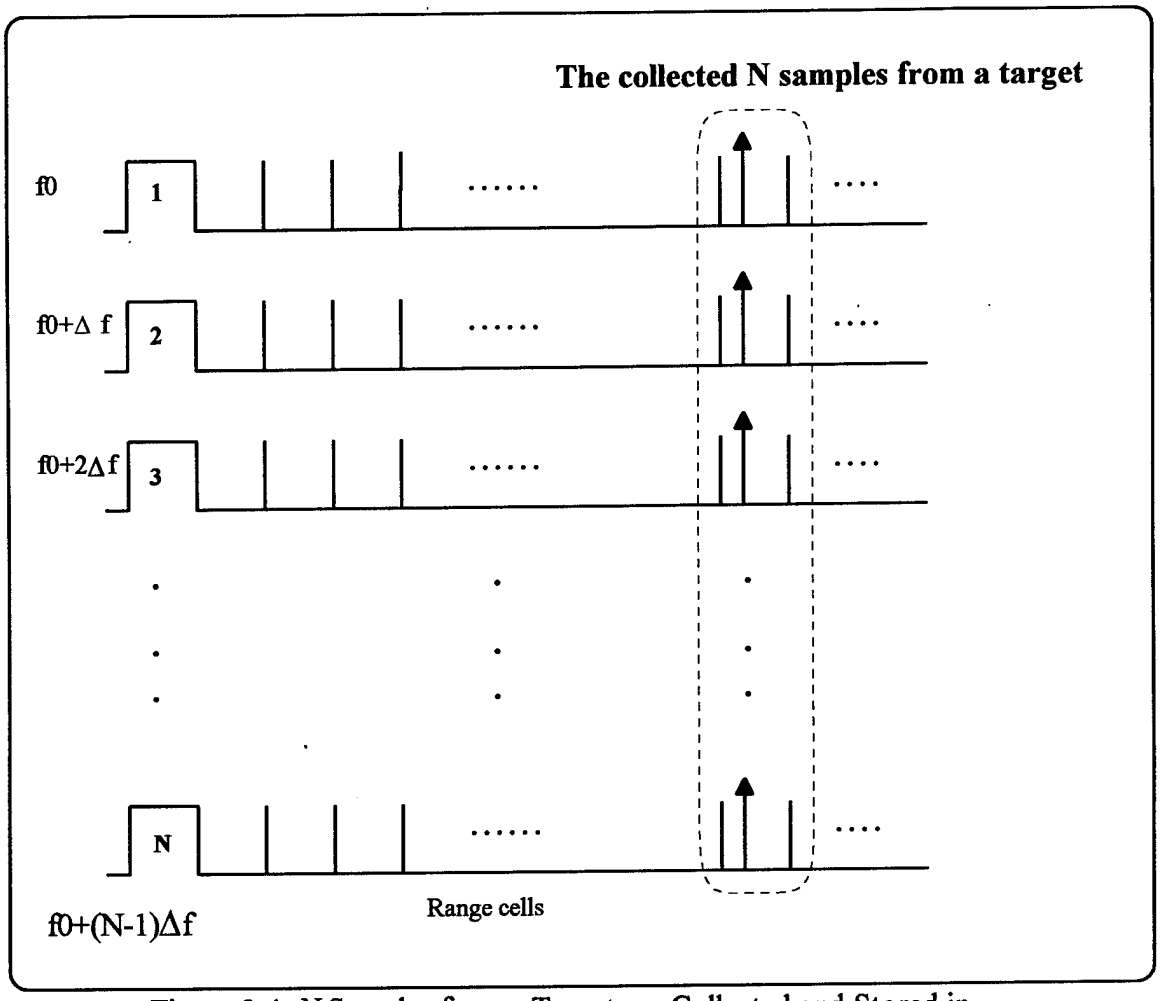

Figure 2.4 *N* Samples from a Target are Collected and Stored in Memory for High Resolution Processing.

For high PRF waveforms, a target echo may arrive in a different PRI. The output of the stepped-frequency synthesizer will have switched to the succeeding stepped-frequencies before receiving and processing the previously transmitted pulses. Two possible solutions to this problem are to switch the synthesizer to the previous transmitted frequencies or to have several synthesizers to sort the multiple-time-around echoes [Ref. 2: p.269].

A key advantage of the stepped-frequency radar over both the ultra-wideband radar and the typical linear frequency-modulated (LFM) pulse compression is the narrowband processing which eliminates requirements for the extremely high A/D sampling rate, a major constraint for conventional pulse compression techniques. The disadvantage of the stepped frequency radar is that it takes longer time to transmit and receive N pulses for high resolution processing. However, in coherent radars, target returns from N transmitted pulses are collected before processing; thus, the stepped-frequency radar does not pose longer delay than the normal coherent radar.

C. HIGH RESOLUTION PROCESSING

The sampled output of the phase detector for the nth pulse can be written as

$$s(n) = a_n \exp(j\phi_n) \tag{2.6}$$

where

ϕ_n = the phase of the nth pulse

a_n = the magnitude of the nth pulse

The phase component of the sampled output for the nth pulse is given by

$$\phi_n = 2\pi f_n \frac{2R_n}{c} \tag{2.7}$$

where f_n is the carrier frequency of the nth pulse given by Eq.2.1, and $2R_n/c$ is the round

trip time of the target return due to the nth pulse. R_n is the range between the target and the radar and is given by

$$R_n = R_0 - (n\text{-}1)vT \tag{2.8}$$

where

R_0 = initial target range

T = pulse repetition interval

v = relative radial velocity between target and radar

By substituting Eq.2.1 and Eq.2.8 for f_n and R_n into Eq.2.7, we obtain

$$\phi_n = 2\pi(f_0 + (n-1)\Delta f)\left(\frac{2(R_0 - (n-1)vT)}{c}\right)$$

$$= \frac{4\pi f_0 R_0}{c} + 2\pi\frac{\Delta f}{T}\frac{2R_0}{c}(n-1)T - 2\pi\frac{2v}{c}f_0(n-1)T$$

$$-2\pi\frac{\Delta f}{T}\frac{2v(n-1)T}{c}(n-1)T \tag{2.9}$$

The expansion of the phase component ϕ_n in above equation contains four terms. The first term of Eq.2.9 is the constant phase resulting from the initial target range and the nominal carrier frequency, and is not of any importance. The second term has an induced frequency shift by the amount of $2\Delta f R_0/Tc$, resulting from the frequency step size during

the round trip time of the initial target range. The third term contains a Doppler frequency shift of the amount $2vf_0/c$ due to the relative radial velocity between the radar and the target. The final term is a frequency dispersion which is determined by the amount of $2v(n\text{-}1)\Delta f/c$ due to the relative radial velocity and the output frequency of the frequency synthesizer. The third and fourth terms of Eq.2.9 are the phase shifts caused by the relative radial velocity between the radar and the target, which will result in target distortion in the range profiles.

1. Generation of HRR profile

After target samples from N pulses are collected, the high range resolution is obtained by coherently processing N samples. In conventional pulsed-Doppler radars, coherent processing is implemented by DFT as a matched filter. Similarly, the high resolution range (HRR) profile in the stepped-frequency radar is obtained by taking the N-point DFT of the collected N target samples, which is written as

$$S(k) = \sum_{n=1}^{N} a_n \exp(j\phi_n)\exp\left(-j\frac{2\pi nk}{N}\right)$$

$$= \sum_{n=1}^{N} a_n \exp(j2\pi f_n \frac{2R_n}{c})\exp\left(-j\frac{2\pi nk}{N}\right) \quad k = 1, 2, \ldots, N \qquad (2.10)$$

Note that the HRR profile maps a specific range cell in which the target is located. Thus, the absolute range of the target is not shown in the HRR profile. Only the relative positions of the scatterers on the target are determined. The DFT bins in the HRR profile

can be interpreted as the relative synthetic range cells which resolve the relative positions of the target scatterers. It is also noted that the same procedure for obtaining the HRR profile can be applied to all other range cells.

To reduce the sidelobe effects in the HRR profile caused by the DFT process, the target signal is multiplied by a weighting function prior to computing DFT. In this thesis, Hamming windows are employed. The weighting function can suppress the range sidelobes of the HRR profile; however, it also causes a degradation of the resolution as indicated by a scaling factor k in the following expression for the range resolution.

$$\Delta r = \frac{kc}{2N\Delta f} \tag{2.11}$$

where

$k = 1.33$ for Hamming window

Note that the DFT process functions as a matched filter for the N target returns due to a burst of N transmitted pulses only in case of zero relative radial velocity between the radar and the target. The non-zero relative radial velocity will result in a mismatch between the DFT and the Doppler-shifted target returns [Ref. 3: p.4]. The result of the mismatch in the DFT process leads to target spreading, shifting and attenuation in the range profile. The target spreading and attenuation are considerably more important than the target shifting because they degrade the desired range resolution and decrease the signal-to-noise ratio. The effects of the relative radial velocity and the required velocity compensation will be discussed in the next section.

2. Maximum Unambiguous Range, R_u

The stepped-frequency radar achieves high range resolution by generating a phase shift by means of linear changes in the carrier frequencies. The induced phase shift due to the frequency change from pulse to pulse is given by the second term of Eq.2.9 as follows

$$\phi_{ind} = 2\pi \frac{\Delta f}{T} \frac{2R_0}{c}(n-1)T \tag{2.12}$$

The induced frequency shift is obtained from above equation by determining the rate of the phase change as

$$f_{ind} = \frac{\Delta f}{T} \frac{2R_0}{c} \tag{2.13}$$

The maximum unambiguous range, R_u is obtained by substituting the maximum induced frequency shift equal to PRF as

$$\text{PRF} = \frac{\Delta f}{T} \frac{2R_u}{c} \tag{2.14}$$

Therefore, the maximum unambiguous range, R_u in the HRR profile is given by

$$R_u = \frac{c}{2\Delta f} \tag{2.15}$$

The fraction of the maximum unambiguous range window R_u occupied by an original range cell ΔR is given by

$$\frac{\Delta R}{R_u} = \frac{c\tau/2}{c/2\Delta f} = \tau\Delta f \tag{2.16}$$

D. EFFECTS OF THE RELATIVE RADIAL VELOCITY

The third and fourth terms in Eq.2.9 are the additional phase shifts due to the relative radial velocity between the radar and the target, resulting in a mismatch in the DFT process. The consequences of the mismatch in the DFT are three negative effects on the range profile. The first effect is target spreading in range. The second effect is the attenuation of target amplitude due to the spreading. The amount of spreading is determined by a dimensionless parameter P given by Eq.2.17 [Ref.2: p.250], which represents the number of the synthetic range cells (or DFT bins) that the target signal spreads in the range profile during the coherent processing interval.

$$P = \frac{vNT}{\Delta r} = \frac{vN}{\Delta r(\mathrm{PRF})} \tag{2.17}$$

The spreading of the target signal results in a loss of synthetic range resolution, for the target signal has broadened from a synthetic range cell with resolution Δr up to several synthetic range cells.

The third effect is the shifting of the target signal in the range profile. The target position will be shifted by L synthetic range cells, where L is given by Eq.2.18 [Ref. 3: p.45].

$$L = \left(\frac{\hat{f}_c}{B_{eff}} \right) P = \frac{\hat{f}_c}{B_{eff}} \frac{vNT}{\Delta r} = \frac{\hat{f}_c}{B_{eff}} \frac{vN}{\Delta r(\mathrm{PRF})} \tag{2.18}$$

where

$$\hat{f}_c = f_0 + \frac{1}{2} B_{eff}$$

If the number of the shifted synthetic range cells L is greater than number of DFT bins, N, the target signal in the range profile will be circularly shifted, resulting in a "wraparound" [Ref. 3: p.41]. The phenomena of the target spreading, shifting and attenuation in the range profile caused by the relative radial velocity are demonstrated in Figure 2.5.

To overcome these drawbacks caused by the relative radial velocity, the received signal can be compensated in phase, which eliminates the effects of the relative radial velocity. This phase compensation depends upon the target velocity and is normally termed as velocity compensation factor. The velocity compensation factor will consist of the third and fourth terms in Eq.2.9 with 180 degrees phase rotation as given by

$$comp(n) = \exp\left(j \frac{4\pi}{c} v(f_0 + (n-1)\Delta f)(n-1)T \right) \tag{2.19}$$

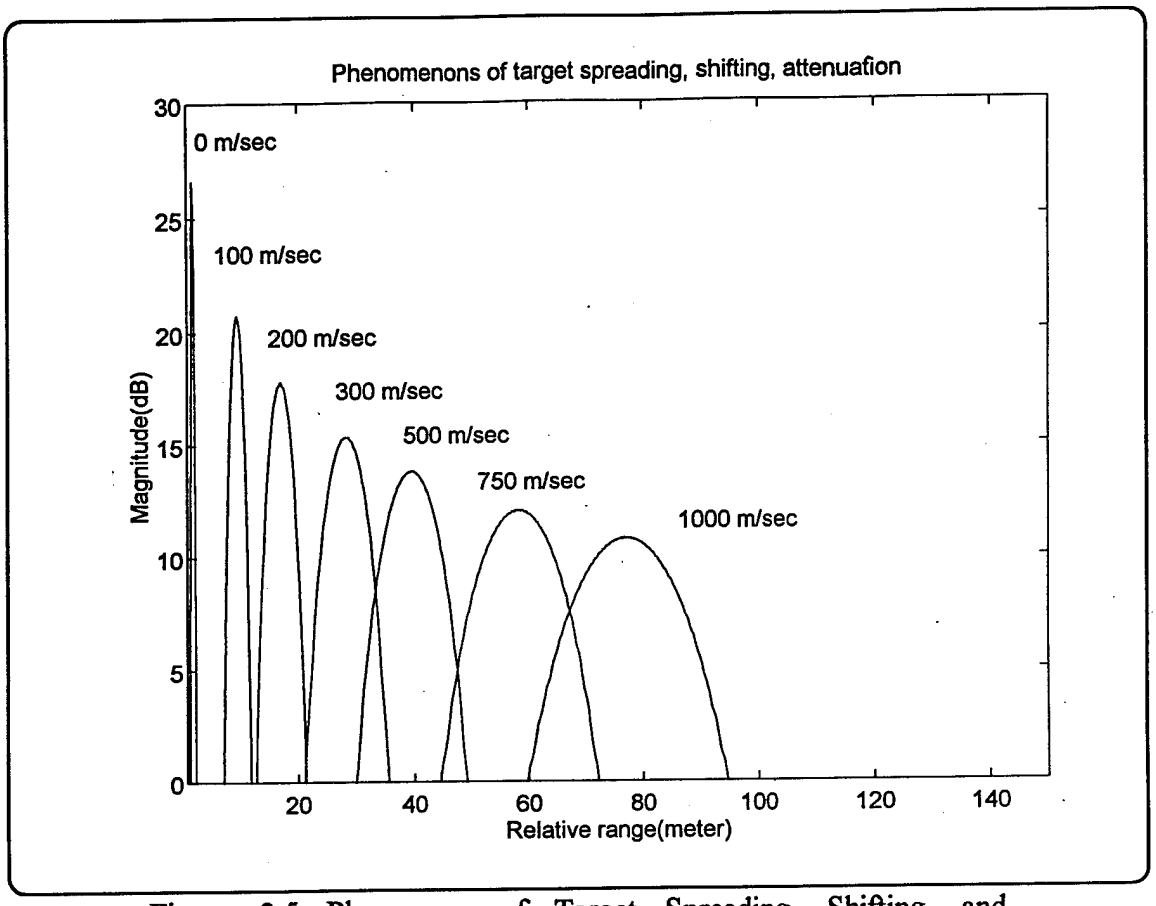

Figure 2.5 Phenomena of Target Spreading, Shifting, and Attenuation for a Single Target Due to Differernt Relative Radial Velocities in the Range Profile. The Target Range is Unchanged. SNR = 13 dB, PRF =20 KHz, f_o = 1GHz, N = 512, Δf = 1 MHz.

With the application of the velocity compensation factor to the received radar signal, the compensated signal becomes

$$C(n) = s(n)\exp\left(j\frac{4\pi}{c}v(f_0 + (n-1)\Delta f)(n-1)T\right) \tag{2.20}$$

where $s(n)$ is given by Eq.2.6.

For a moving target in clutter, with DFT processing, the moving target shifts from the clutter-filled region to the clutter-free region in the HRR profile as shown in Figure 2.6. However, the straightforward application of the velocity compensation factor to the received radar signal will simply compensate the target signal, but the clutter will spread in the range profile due to the unnecessary compensation velocity. Thus, clutter cancellation should be done before applying the velocity compensation factor in a velocity compensation scheme. The detailed study of the velocity compensation scheme for a moving target detection in clutter using the stepped-frequency waveform will be discussed in Chapter III.

E. SELECTION OF PULSE WIDTH, τ AND FREQUENCY STEP SIZE, Δf

The design of a stepped-frequency radar system requires a thorough understanding of the effects of the primary waveform parameters on the system performance. The selection of the primary waveform parameters, such as the pulse width, τ and the frequency step size, Δf, are important in the system design. The selection of pulse width, τ depends on the maximum target extent, E. One basic requirement for good target

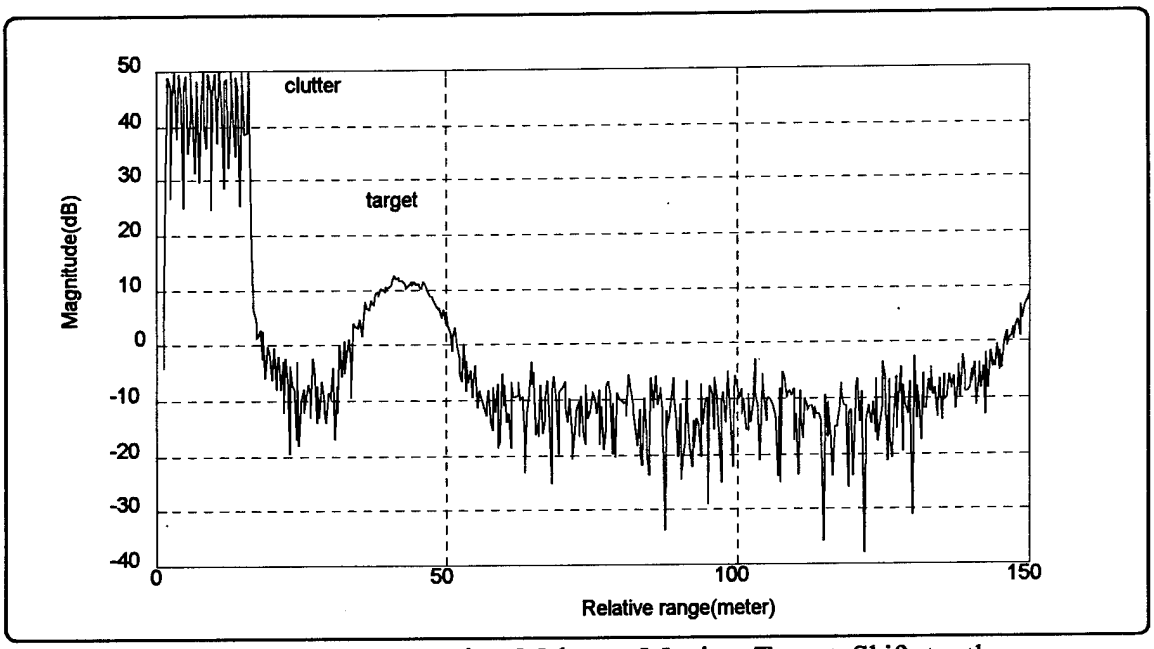

Figure 2.6 DFT Processing Makes a Moving Target Shift to the Clutter-Free Region in the Range Profile. The Relative Radial Velocity = 500 m/sec, PRF = 20 KHz, f_0 = 10GHz, N = 512, Δf = 1 MHz, CNR = 35 dB, SNR =11 dB.

delectability is that the pulse width must encompass the maximum target extent. This means that the pulse width, τ must be greater than or equal to the round trip time for length E.

$$\tau \geq \frac{2E}{c} \tag{2.21}$$

or

$$E \leq \frac{c\tau}{2} \tag{2.22}$$

If the pulse width cannot encompass the target extent (in range), different scatterers on a target will not be located within the same original range cell, resulting in a loss of *SNR* and an incomplete HRR profile.

The requirement in choosing the frequency step size Δf is that the maximum unambiguous range window R_u must encompass the maximum target extent E to avoid target wraparound. That is,

$$R_u = \frac{c}{2\Delta f} \geq E \tag{2.23}$$

or

$$\Delta f \leq \frac{c}{2E} \tag{2.24}$$

When dealing with moving target detection in clutter, the maximum unambiguous range window, R_u should be much greater than the original range cell, ΔR in which the target is contained. That is,

$$R_u = \frac{c}{2\Delta f} >> \Delta R = \frac{c\tau}{2} \tag{2.25}$$

or

$$\tau\Delta f << 1 \tag{2.26}$$

Thus, the unused portion of the HRR profile is a clutter-free region which can be used to detect the shifted target signal. In this situation, the original range cell, ΔR will comprise only a small fraction of the maximum unambiguous range window, R_u.

When $\tau\Delta f = 1$, the maximum unambiguous range window, R_u is equal to an original range cell, ΔR. In this situation, it is difficult to notice the target wraparound caused by slight changes in the target range. Furthermore, aliasing may occur if there is interference from adjacent range cells. If the original range cell encompasses the target and the clutter, the target will be camouflaged by the clutter [Ref. 1: p.168]. Thus, the condition of $\tau\Delta f = 1$ is only effective for target detection in a non-clutter environment.

When $\tau\Delta f > 1$, the maximum unambiguous range window, R_u is smaller than the original range cell, ΔR. As a result, the region of the original range cell not contained within the maximum unambiguous range window will fold over and result in aliasing. This situation must be avoided for mapping HRR profiles [Ref. 6: p.602-603].

(This page is intentionally left blank.)

III. VELOCITY COMPENSATION IN THE STEPPED FREQUENCY RADAR

Velocity compensation plays an important role in the stepped-frequency radar system, for the resolution in the range profile degrades when there is a non-zero relative radial velocity between the radar and the target. A target in presence of clutter can be clearly seen only when sufficient relative radial velocity makes the target shift into the clutter-free region in the range profile. With DFT processing, the moving target spreads in range and attenuates in magnitude. The target spreading factor P given by Eq.2.17 determines the number of the synthetic range cells occupied by the moving target in the range profile. The effective synthetic resolution for a moving target is $P\Delta r$ instead of the theoretical resolution, Δr. In addition to the loss of range resolution, the excessive target shift due to the relative radial velocity may result in target wraparound. The number of synthetic range cells that a moving target shifts in the range profile is equal to the target shifting factor, L given by Eq.2.18.

In order to overcome the drawbacks of target spreading and attenuation due to the relative radial motion between the radar and the target, the velocity compensation factor given by Eq.2.19 can be directly applied to the received radar signal. However, this will simply compensate the target signal, while the clutter spreads in the range profiles due to the unnecessary compensation velocity. Thus, in a velocity compensation scheme, the clutter cancellation process should be done prior to applying the velocity compensation factor.

Three velocity compensation schemes are designed and discussed in this chapter. In the first and the second schemes, the relative radial velocity is assumed to be known in advance. The third scheme deals with the target of unknown velocity, but the velocity is assumed within a defined interval. Computer simulations for the three compensation schemes are also presented in this chapter.

A. VELOCITY COMPENSATION SCHEME 1

The first compensation scheme for detection of moving targets in clutter is shown in Figure 3.1. In this scheme, the received return signal in the time domain is first windowed prior to taking the DFT. This DFT process generates the uncompensated range profile. At this stage, the clutter occupies $N(\tau\Delta f)$ synthetic range cells, which is canceled by multiplying by a rectangular gating function. The modified range profile is then transformed back to the time domain signal by an inverse DFT (IDFT). The velocity compensation factor is now applied to the clutter-canceled target signal in the time domain. After velocity compensation, the target signal is windowed and the DFT is performed once again. This final DFT generates a clutter-free and velocity-compensated HRR profile.

Note that in this scheme, two weighting functions are employed to reduce the range sidelobes caused by the DFT process. The first weighting function is necessary, and the second weighting function gives a minor improvement in the range resolution.

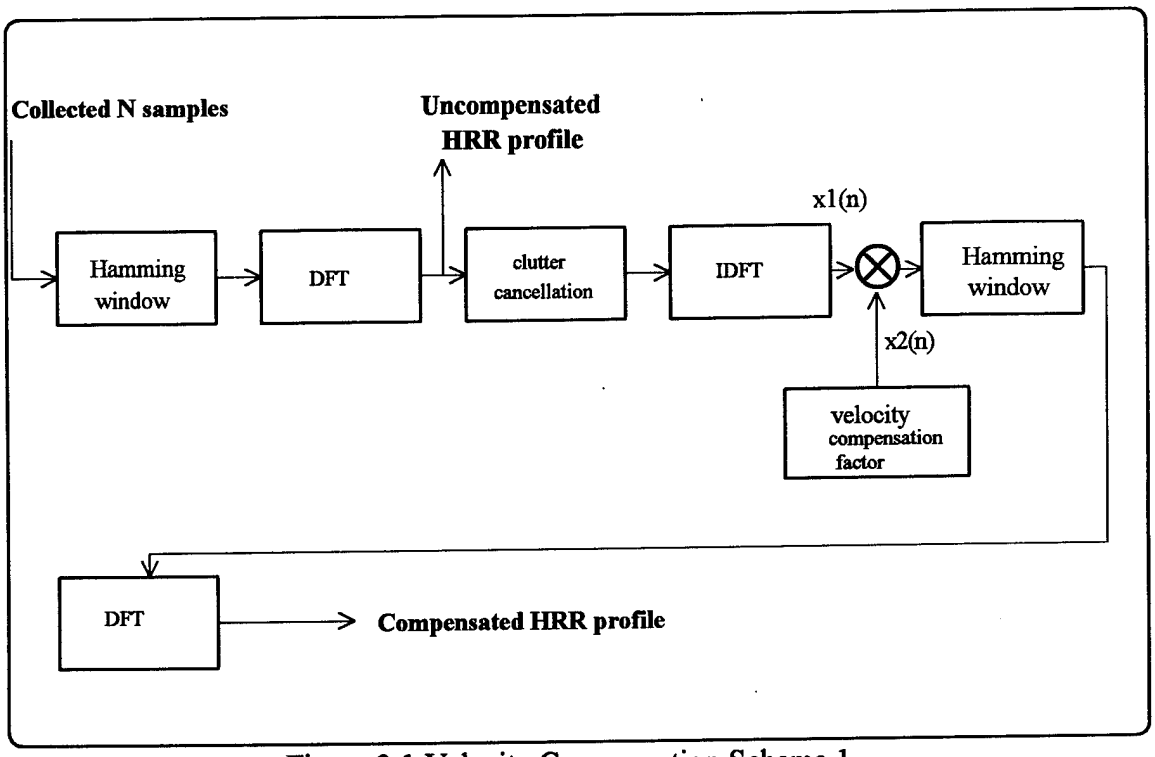

Figure 3.1 Velocity Compensation Scheme 1.

B. VELOCITY COMPENSATION SCHEME 2

In this section, an alternative scheme is developed for velocity compensation. This new scheme is based on *frequency convolution* [Ref. 4: p.427] which is shown in Figure 3.2 and written as

$$[x_1(n) \bullet x_2(n)] = \frac{1}{N} \text{IDFT}[X_1(k) * X_2(k)] \tag{3.1}$$

where $x_1(n)$ and $x_2(n)$ are finite duration time domain sequences both having the same length N, while $X_1(k)$ and $X_2(k)$ are the DFTs of $x_1(n)$ and $x_2(n)$, having the same length N. Note that the convolution in the frequency domain is a circular convolution, not the

common linear convolution. Thus, the result of frequency convolution will also be a sequence of length N.

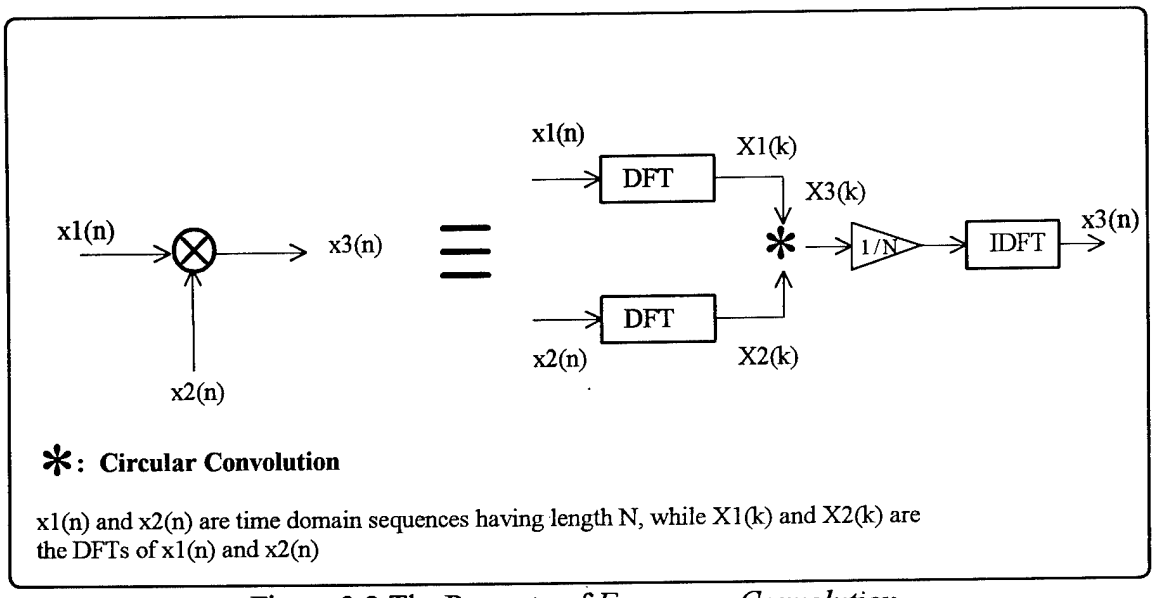

Figure 3.2 The Property of *Frequency Convolution*.

In Figure 3.1, the product of $x_1(n)$ and $x_2(n)$ is replaced by the circular convolution of $X_1(k)$ and $X_2(k)$ and the succeeding IDFT, where $x_1(n)$ represents the output of the IDFT and $x_2(n)$ represent the velocity compensation factor. Thus, the first scheme is expanded as shown in Figure 3.3. The purpose of this substitution is to cancel out the two operations of IDFT and DFT in Figure 3.1, resulting in a modified scheme as shown in Figure 3.4. The cancellation of these operations is expected to speed up the computation.

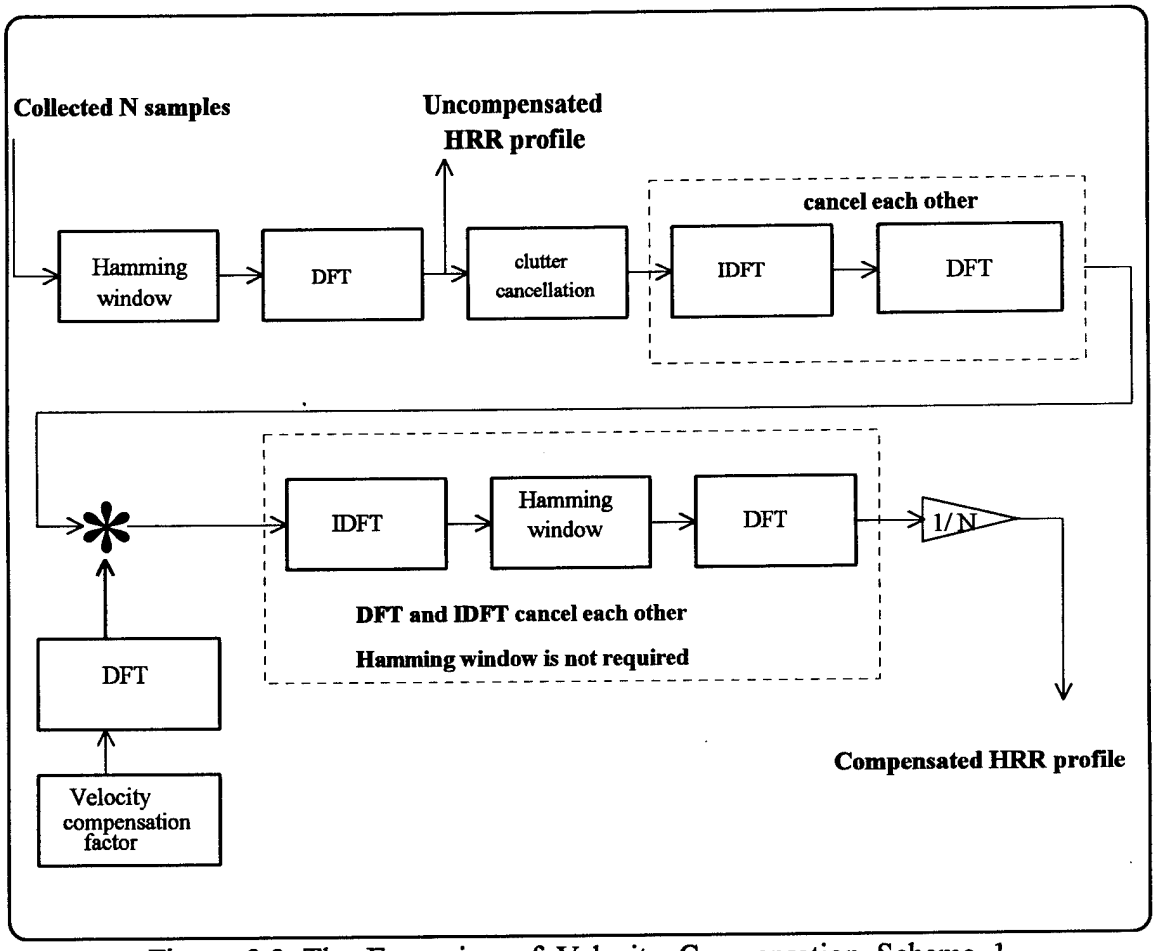

Figure 3.3 The Expansion of Velocity Compensation Scheme 1 According to *Frequency Convolution*.

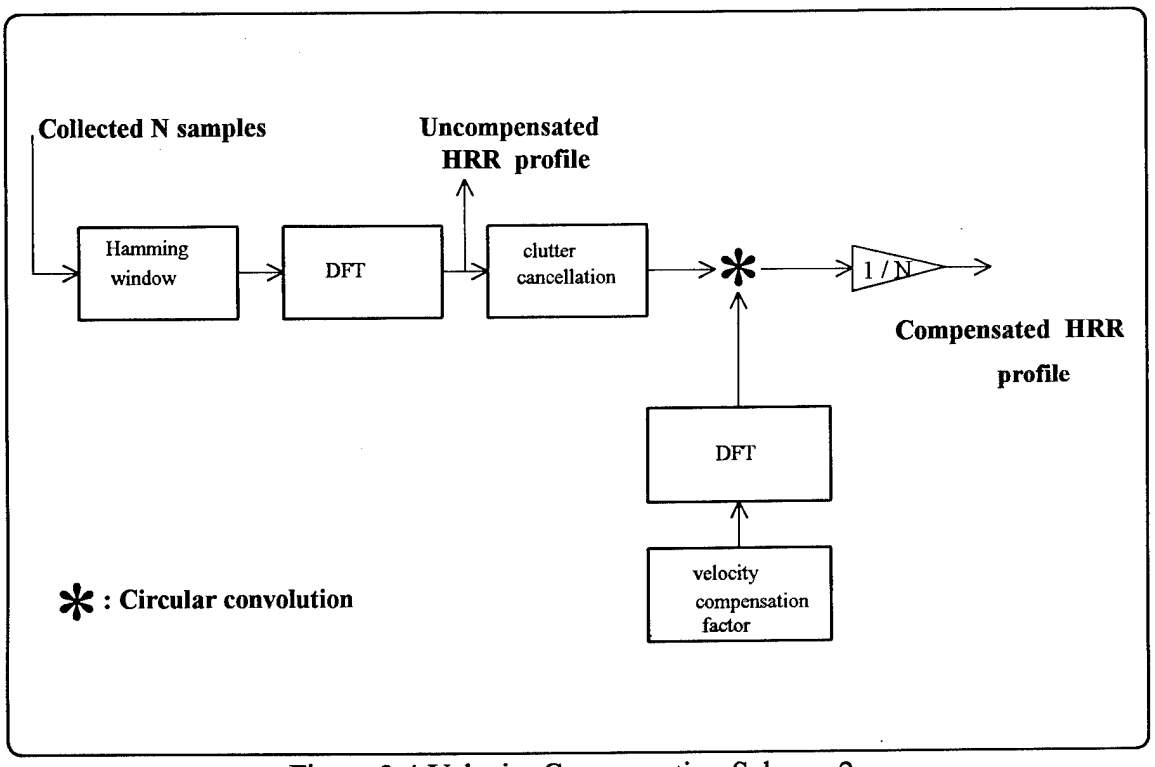

Figure 3.4 Velocity Compensation Scheme 2.

C. ANALYSIS AND COMPARISON OF SCHEME 1 AND SCHEME 2

Both velocity compensation schemes are functionally equivalent. In structure, the major difference between the two schemes is that in scheme 1, the velocity compensation is done by multiplication in the time domain, while in scheme 2, the velocity compensation is done by circular convolution in the frequency domain. As a basis for comparison, we will use the number of complex multiplies required in each scheme as a measure of computational complexity.

In scheme 1 (shown in Figure 3.1), there are two Hamming windows, three DFT processes (including IDFT), one clutter cancellation filter, and one complex multiplication with the velocity compensation factor. Assume that there are N samples for the receive

signal and N is a power of 2. The DFT process of scheme 1 is achieved by the Fast Fourier Transform (FFT) algorithm. Thus, there are N complex multiplies in each Hamming window, $(N/2)\log_2 N$ complex multiplies in each DFT process [Ref. 4: p.506], N complex multiplies in the clutter cancellation and N complex multiplies in the multiplication with the velocity compensation factor. There are a total of $(3N/2)\log_2 N + 4N$ complex multiplies involved in scheme 1 provided that an FFT algorithm is employed in the DFT process. For example, when $N = 512$, there will be a total of 8960 complex multiplies required in scheme 1. If the DFT process is not implemented by an FFT algorithm, but by the standard DFT algorithm, there will be N^2 complex multiplies in each DFT process [Ref. 4: p.426]. Thus, there will be a total of $3N^2 + 4N$ complex multiplies involved in scheme 1. When $N = 512$, there are a total of 788,480 complex multiplies required (approximately 88 times the computational cost of using the FFT algorithm). Therefore, the FFT algorithm used in the DFT process of scheme 1 can provide much higher computational speed than the standard DFT algorithm.

In scheme 2 (shown in Figure 3.4), we can find one Hamming window, two DFT processes, one clutter cancellation filter and one circular convolution with the velocity compensation factor in the frequency domain. A direct approach for the circular convolution process requires N^2 complex multiplies [Ref. 4: p.426]. Assume that the FFT algorithm is used in the DFT process of scheme 2. Thus, there are a total of $(N \log_2 N) + 2N + N^2$ complex multiplies. When $N = 512$, there will be 267,776 complex multiplies required in scheme 2, which are much more than those required for the FFT algorithm in

scheme 1. If the standard DFT algorithm is employed in scheme 2, there will be a total of $3N^2 + 2N$ complex multiplies. Thus, for $N = 512$, there are 787,456 complex multiplies required, which is about the same computational complexity as using the standard DFT algorithm in scheme 1. As expected, for both velocity compensation schemes, the FFT algorithm will offer less computational complexity and higher processing speed than the standard DFT algorithm.

From the previous analysis, it is found that when the FFT algorithm is employed in the DFT process of both schemes, the circular convolution will be the major factor that results in the much greater computational complexity in scheme 2. Therefore, scheme 1 mechanized with the FFT algorithm is recommended for velocity compensation in the stepped-frequency radar.

D. VELOCITY COMPENSATION SCHEME 3

The third scheme is proposed to deal with the target of unknown velocity. However, the target velocity is assumed within a defined interval. Scheme 3, as shown in Figure 3.5 is implemented by using the model of scheme 1 or scheme 2, with the addition of a velocity compensation loop. Scheme 1 is employed here as the base model because it has much higher processing speed than scheme 2. In scheme 3, the stepped-frequency radar will automatically try several compensation velocities to generate compensated HRR profiles. These compensated HRR profiles will be stored in memory and compared to find the one with the best resolution and signal-to-noise ratio (*SNR*). It should be noted that in scheme 3, the compensation velocities which begin at a defined initial value are

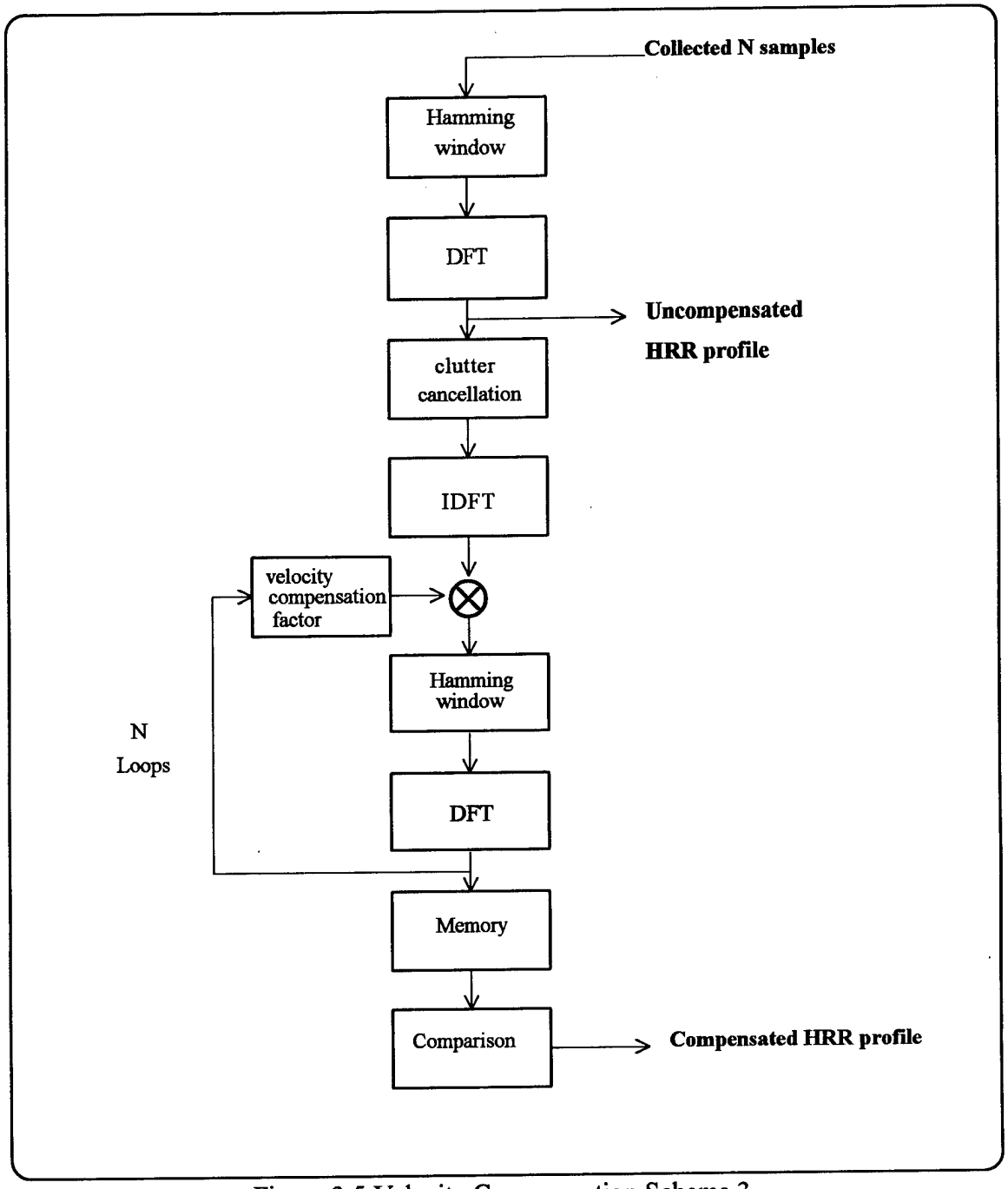

Figure 3.5 Velocity Compemsation Scheme 3.

monotonically increased by a velocity step size, Δv in each loop. The selection of velocity step size, Δv and the number of compensation loops will depend on the size of the defined velocity interval and the waveform parameters.

E. SIMULATION

Scenario: A moving target approaches a surface-based stepped-frequency radar at nose aspect as shown in Figure 3.6. The radar platform and the clutter are assumed stationary. The target with four dominant scatterers on it, is 8 m long at a distance of 11250 m from the radar. The ranges of the scatterers on the target are 11251 m for scatterer 1 (RCS = 0.6 m^2), 11253 m for scatterer 2 (RCS = 0.5 m^2), 11255 m for scatterer 3 (RCS = 1 m^2) and 11257 m for scatterer 4 (RCS = 0.7 m^2). The relative radial velocity between the target and the radar is initially assumed to be 750m/sec, and will be varied in the simulation for the purpose of testing the effects of the relative radial velocity. The clutter-to-noise ratio (CNR) is 35 dB. The variance of the thermal noise which is modeled as white Gaussian noise is set to 0.0002. The signal-to-noise ratio (SNR), 13 dB is based on the power ratio of scatterer 3 (RCS = 1 m^2) to the thermal noise.

Waveform parameters used in the simulation are as follows.

Number of pulses per burst (N):	512
Nominal carrier frequency (f_0):	10 GHz
Frequency step size (Δf):	1 MHz
Pulse repetition frequency (PRF):	200 KHz
Pulse width (τ):	0.1 μsec

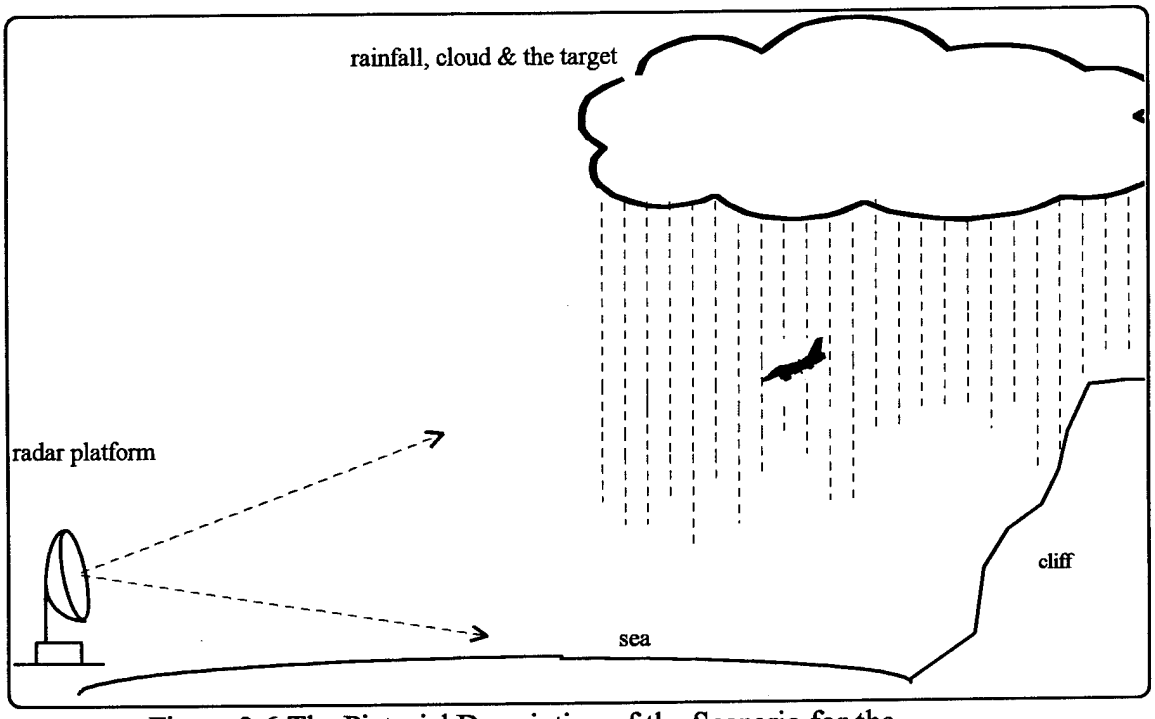

Figure 3.6 The Pictorial Description of the Scenario for the Detection of a Moving Target in Clutter.

Calculations of pertinent quantities are as follows.

Total effective bandwidth:

$$B_{eff} = N\Delta f = 500 \times 1 \text{ MHz} = 512 \text{ MHz}$$

Maximum unambiguous range in the HRR profile:

$$R_u = \frac{c}{2\Delta f} = \frac{3 \times 10^8 \text{ m/sec}}{2 \times 10^6 \text{ Hz}} = 150 \text{ m}$$

Original range cell size:

$$\Delta R = \frac{c\tau}{2} = \frac{(3 \times 10^8 \text{ m/sec}) \times (0.1 \times 10^{-6} \text{sec})}{2} = 15 \text{ m}$$

Synthetic range cell size:

$$\Delta r = \frac{c}{2B_{eff}} = \frac{c}{2N\Delta f} = \frac{R_u}{N} = 0.293 \text{ m}$$

The fraction of R_u occupied by ΔR:

$$\frac{\Delta R}{R_u} = \frac{c\tau/2}{c/2\Delta f} = \tau\Delta f = 0.1$$

The number of synthetic range cells within the fraction of ΔR in the HRR profile:

$$\frac{\Delta R}{R_u} \times N = (\tau\Delta f) \times N = 0.1 \times 512 = 51.2 \approx 52$$

Frequency resolution of DFT:

$$\frac{1}{N \times \text{PRI}} = \frac{\text{PRF}}{N} = \frac{200 \times 10^3 \text{ Hz}}{500} = 390.625 \text{ Hz}$$

The maximum unambiguous range, R_u of the HRR profile and its corresponding maximum induced frequency, PRF, in the DFT is described in Figure 3.7. Simulation programs are written in MATLAB where the DFT process is computed by using a radix-2 FFT algorithm when the length of the sequence is a power of 2 [Ref.5: p.271].

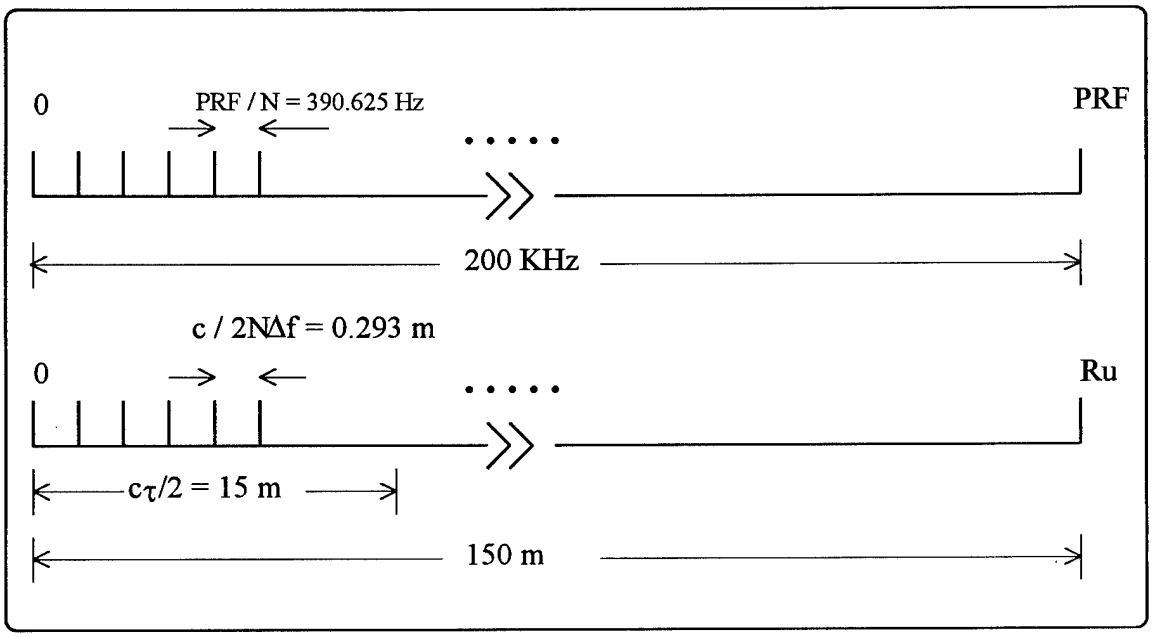

Figure 3.7 The Maximum Unambiguous Range, R_u in the HRR Profile is Equivalent to the Maximum Induced Frequency Shift, PRF.

1. Effects of The Relative Radial Velocity

To demonstrate effects of the relative radial velocity in the range profiles clearly, the relative radial velocity is varied in each uncompensated range profile. The relative radial velocities to be tested in this simulation are 0 m/sec, 350 m/sec, 650 m/sec, 950 m/sec and 1250 m/sec. The simulation results are shown in Figure 3.8 through Figure 3.12.

In Figure 3.8, the target signal is in clutter and cannot be detected since there is no relative radial velocity between the target and the radar. In Figure 3.9, the target signal from a moving target shifts from the clutter-filled region to the clutter-free region, but the magnitude of target signal is much smaller than that of the clutter. Thus, the target will possibly be treated as noise and neglected. As shown in Figure 3.10 through 3.12, the scatterers on the target cannot be resolved, and the phenomena of the target spreading, shifting, and signal attenuation in the range profiles become more prominent as the relative radial velocity increases. It is also noted that in Figure 3.9, the relative radial velocity is 350 m/sec, but the scatterers on the target can still be resolved because the use of a high PRF (200 KHz) reduces target spreading.

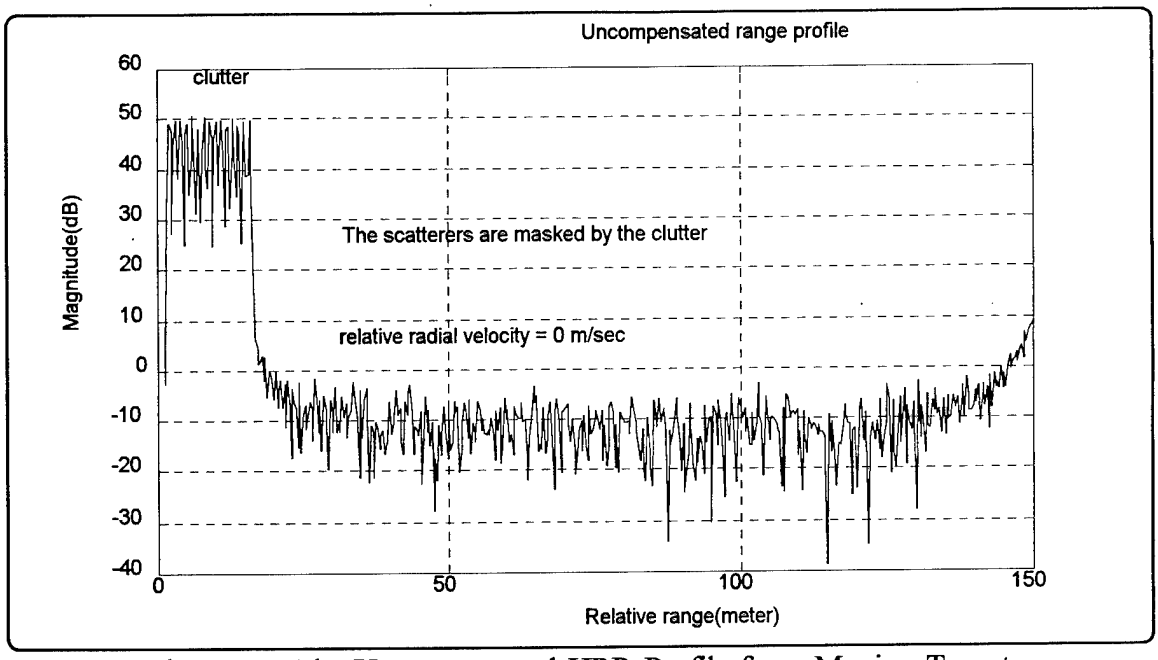

Figure 3.8 The Uncompensated HRR Profile for a Moving Target with Scatterers in Clutter. The Target are Masked by the Clutter Since There is No Relative Radial Velocity between the Radar and the Target.

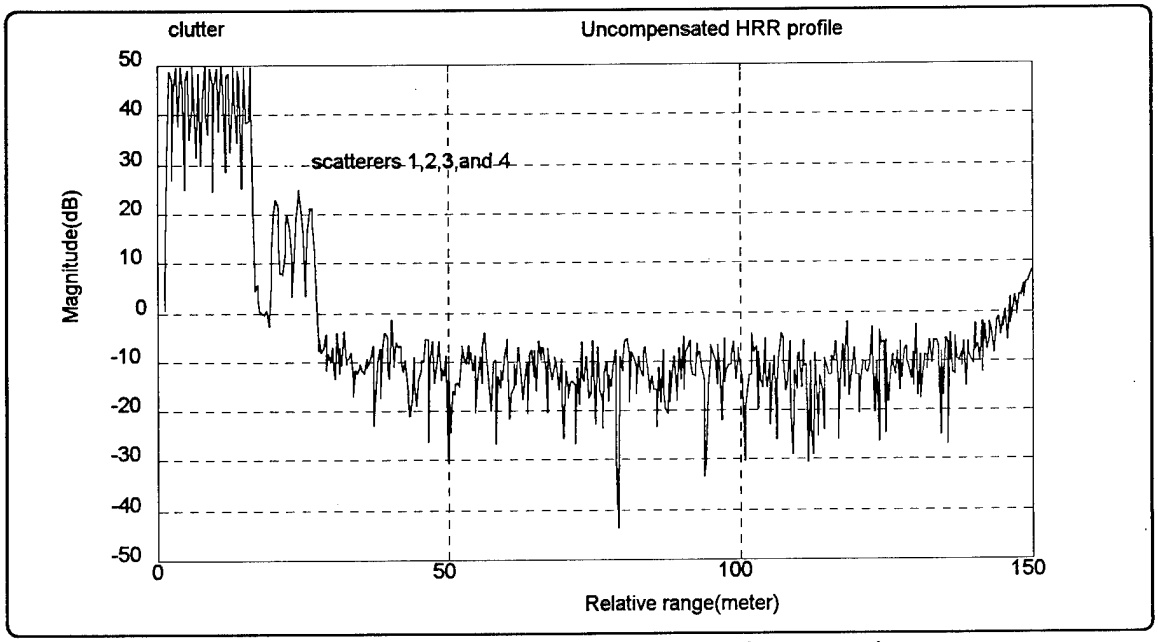

Figure 3.9 The Uncompensated HRR Profile for a Moving Target with Scatterers in Clutter. The Relative Radial Velocity = 350 m/sec.

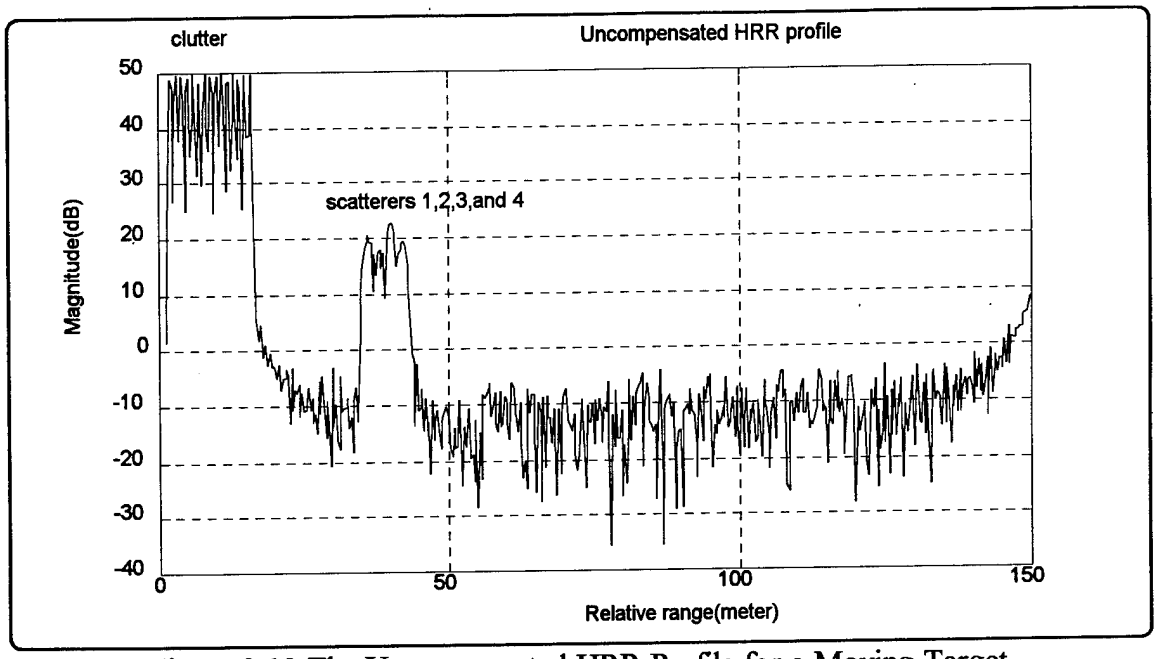

Figure 3.10 The Uncompensated HRR Profile for a Moving Target with Scatterers in Clutter. The Relative Radial Velocity = 650 m/sec.

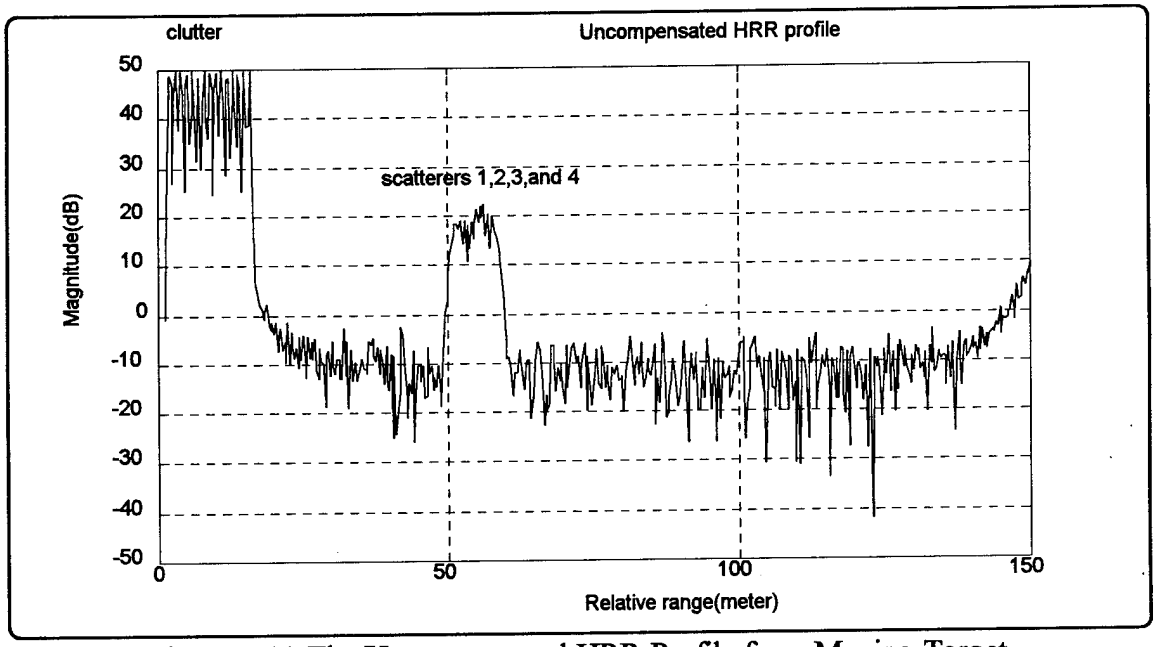

Figure 3.11 The Uncompensated HRR Profile for a Moving Target with Scatterers in Clutter. The Relative Radial Velocity = 950 m/sec.

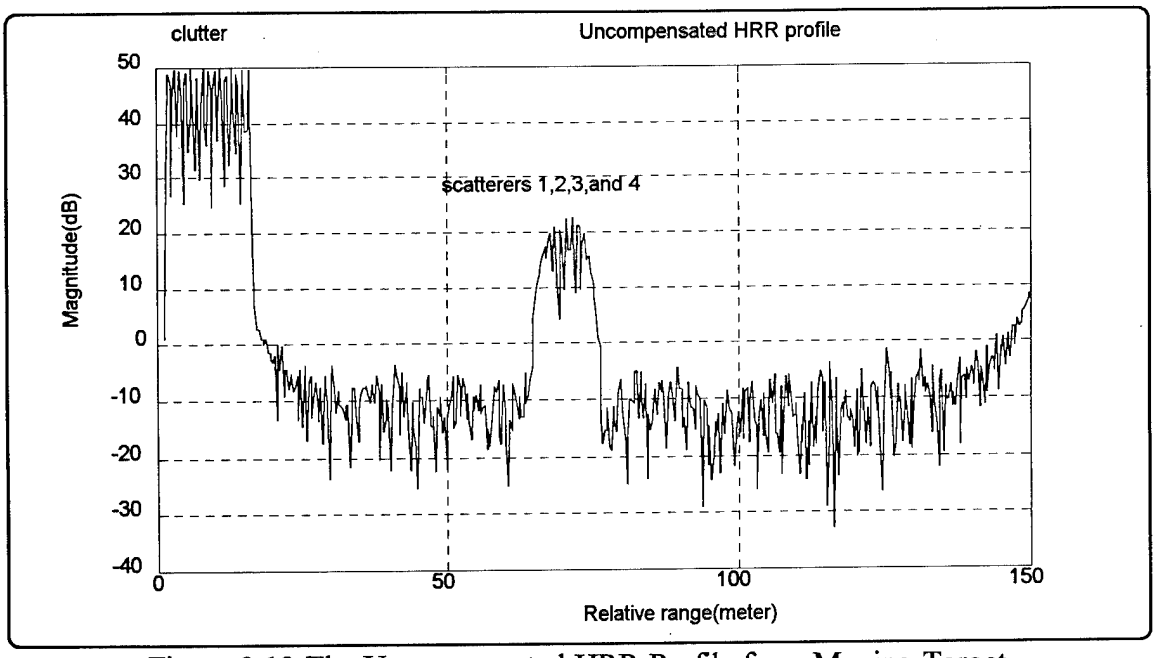

Figure 3.12 The Uncompensated HRR Profile for a Moving Target with Scatterers in Clutter. The Relative Radial Velocity = 1250 m/sec.

2. Simulation of Scheme 1 And Scheme 2

In this subsection, velocity compensation scheme 1 and scheme 2 designed for the detection of a moving target in clutter are simulated. The radar parameters given in the scenario are used in the simulation. The relative radial velocity between the radar and the target is 750 m/sec, and the PRF is 200 KHz. Several compensation velocities, such as 150 m/sec, 350 m/sec, 550 m/sec, 750 m/sec, 1000 m/sec, and 1250 m/sec, are used to evaluate the performance of both compensation schemes. When the compensation velocity is equal to 750 m/sec, the range profile is correctly compensated. The uncompensated range profile is shown in Figure 3.13. The simulation results for compensated profiles are shown in Figure 3.14 through Figure 3.25.

In Figure 3.14 through Figure 3.25, the clutter has been canceled and the target resolution becomes finer as the compensation velocities get closer to the relative radial velocity, 750 m/sec. In the correctly compensated HRR profiles shown in Figure 3.17 and Figure 3.22, the scatterers on the target are the most clearly resolved and have the best *SNR*, for the relative radial velocity is fully compensated, and hence, the DFT process functions as a matched filter to the received signal. Also, the *SNR* (based on the third target scatterer to thermal noise) in the fully compensated HRR profiles is almost up to 30 dB which is much higher than the previously given 13 dB. This increased *SNR* is due to the coherent integration of N pulses in the DFT process.

Note that in some of the HRR profiles without correct velocity compensation, for example, those shown in Figures 3.16, 3.18 , 3.21, and 3.23, the scatterers on the target can still be distinguished because the PRF used in the simulation has a high value of 200 KHz which leads to lower target dispersion. It is also observed from Figures 3.18 and 3.23 that the target signal is circularly shifted to the other edge in the range profile due to the excessive compensation velocity.

In general, the first scheme and the second scheme generate very similar compensated HRR profiles for the same compensated velocity. Nevertheless, comparing the simulation results of both schemes carefully, it is found that the compensated HRR profiles generated by scheme 2 have higher range sidelobes and noise ripples. The lower range sidelobes in the compensated HRR profiles generated by scheme 1 are due to the existence of one more Hamming window in the scheme.

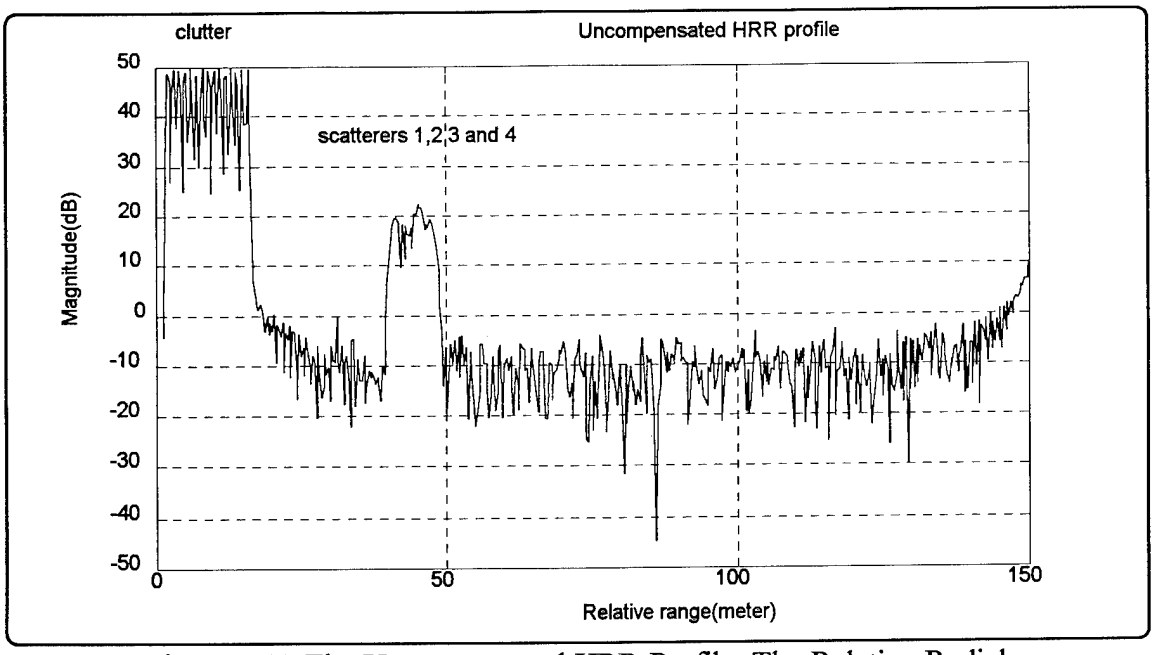

Figure 3.13 The Uncompensated HRR Profile. The Relative Radial Velocity = 750 m/sec.

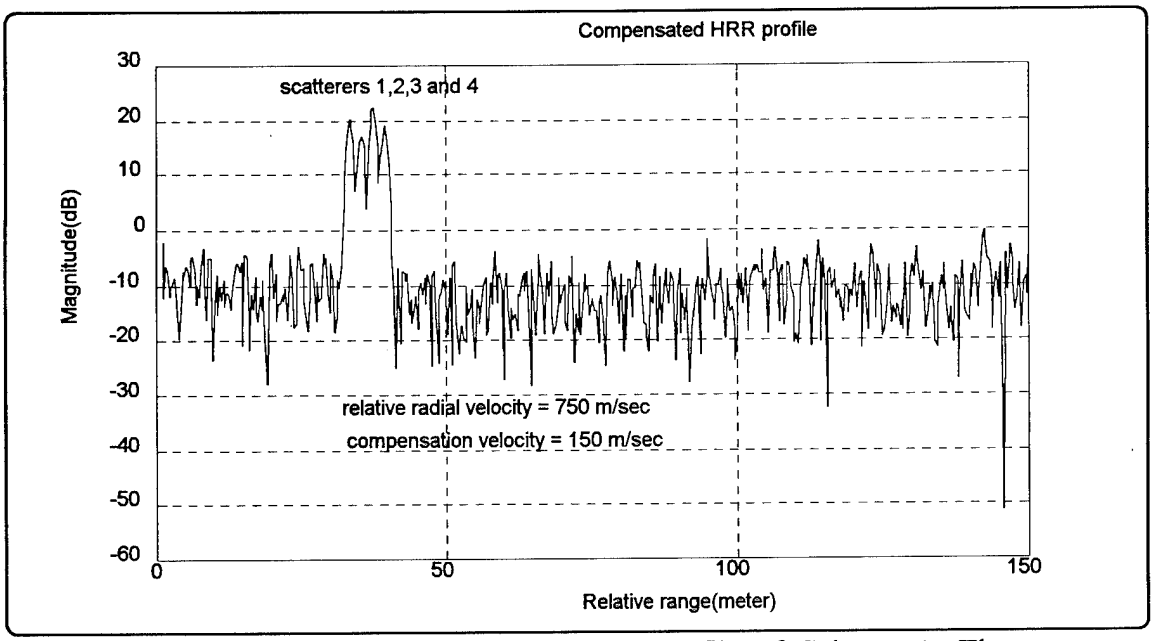

Figure 3.14 The Compensated HRR Profile of Scheme 1. The Clutter is Canceled. Compensation Velocity = 150 m/sec.

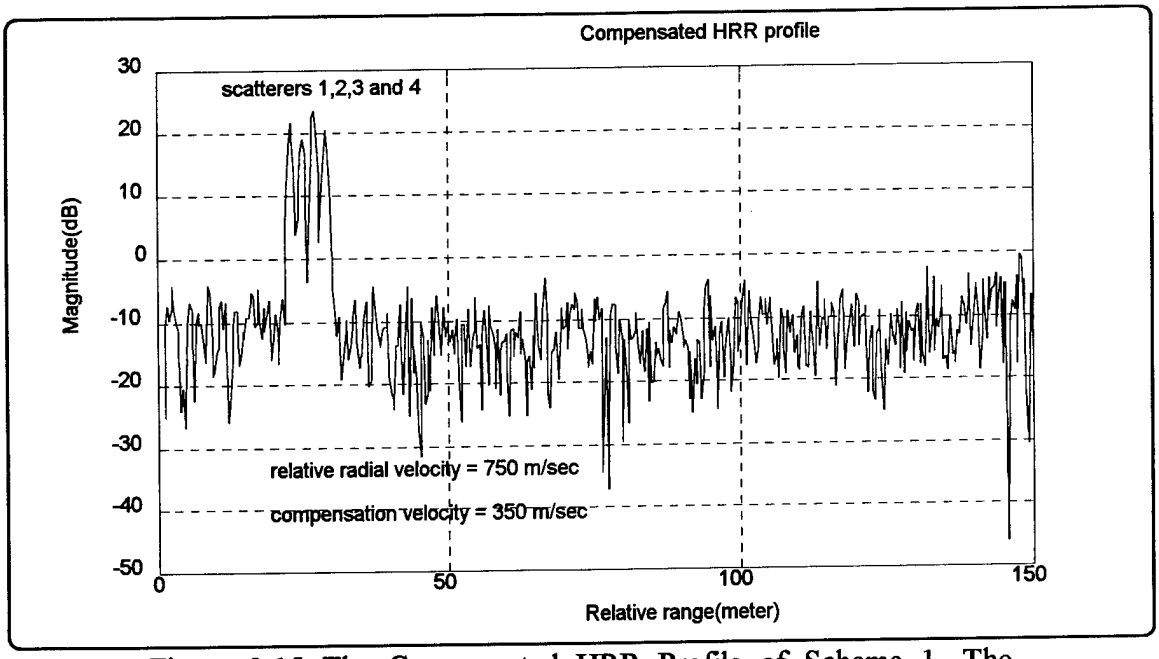

Figure 3.15 The Compensated HRR Profile of Scheme 1. The Clutter is Canceled. Compensation Velocity = 350m/sec.

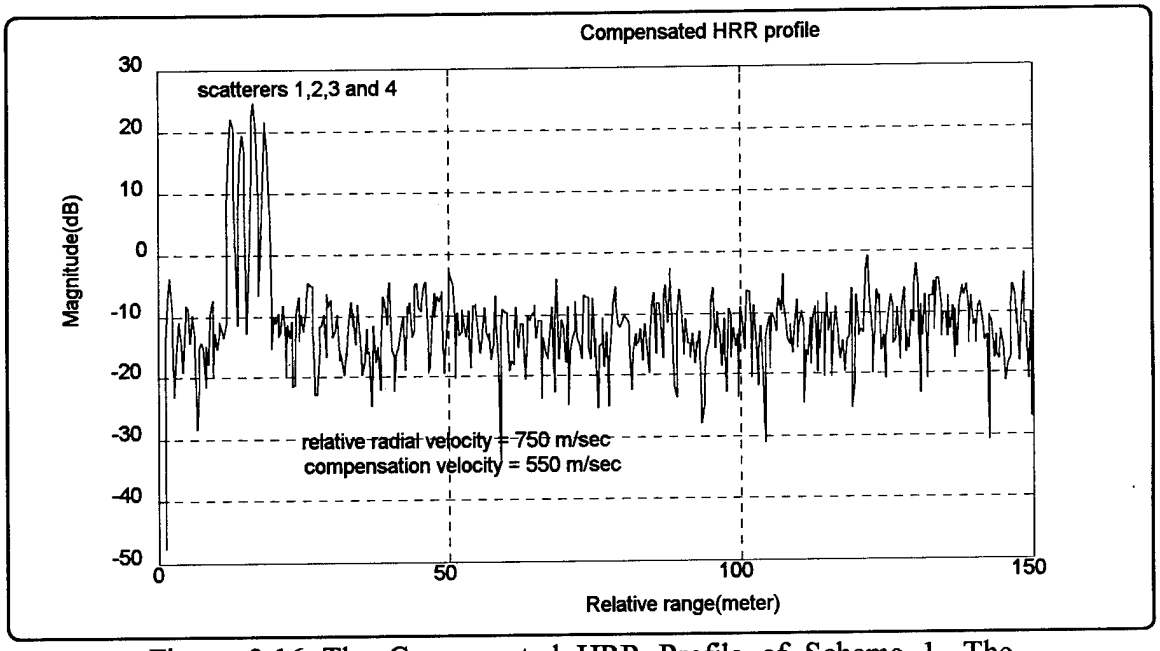

Figure 3.16 The Compensated HRR Profile of Scheme 1. The Clutter is Canceled. Compensation Velocity = 550m/sec.

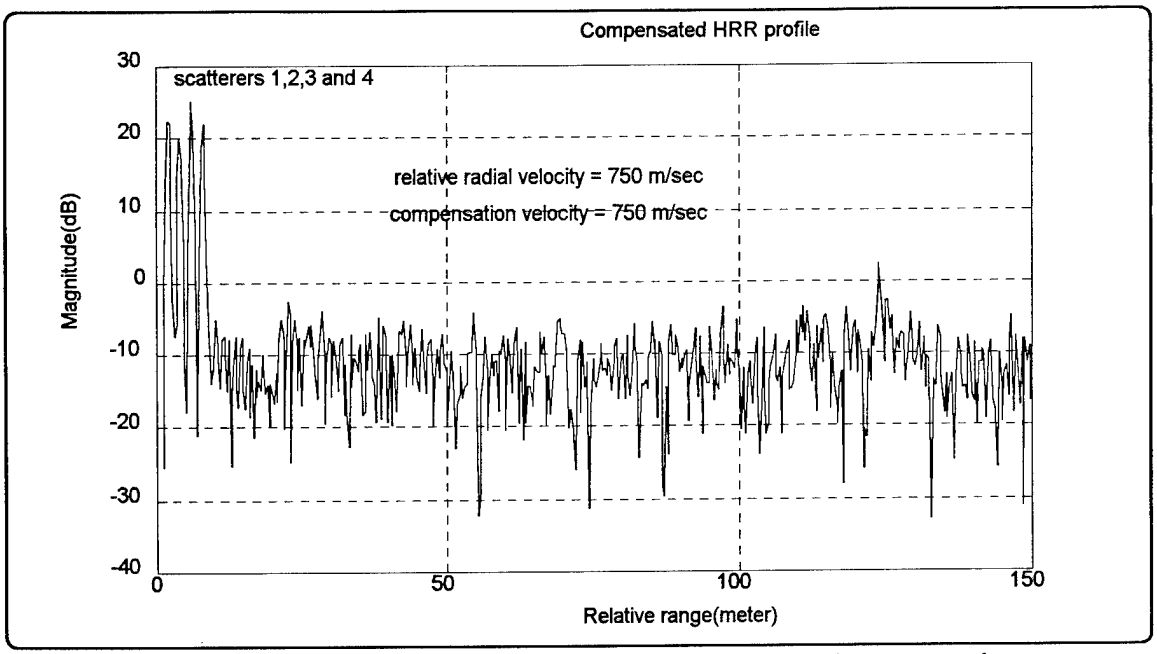

Figure 3.17 The Compensated HRR Profile of Scheme 1. The Clutter is Canceled. Compensation Velocity = 750 m/sec. Note That This is a Correctly Velocity-Compensated HRR Profile.

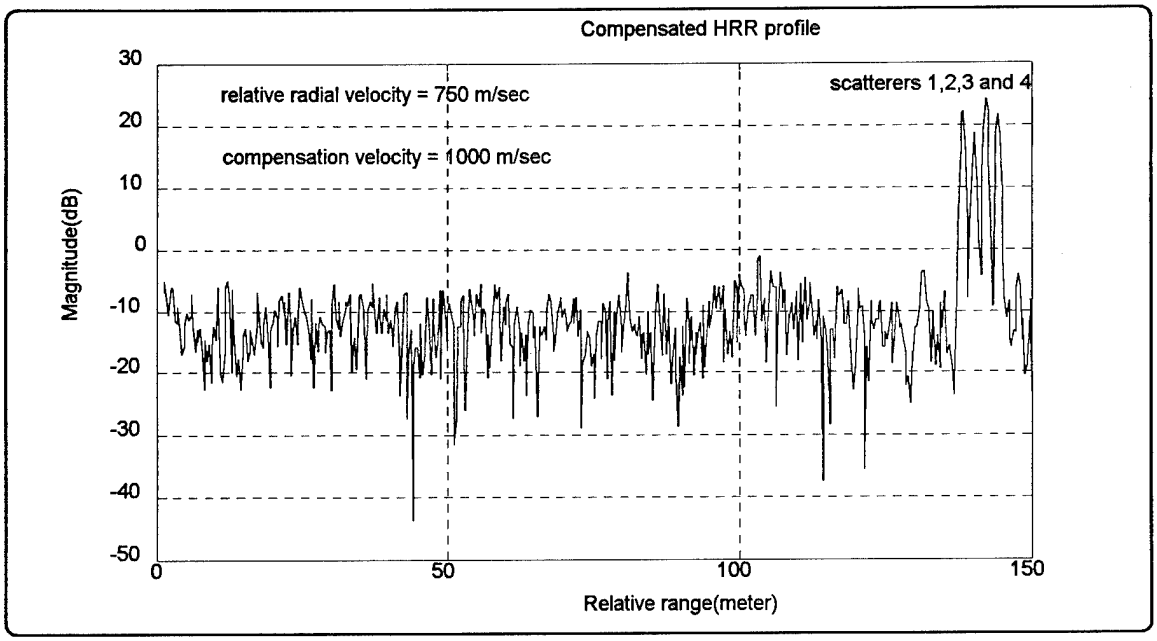

Figure 3.18 The Compensated HRR Profile of Scheme 1. The Clutter is Canceled. Compensation Velocity = 1000 m/sec. The Target Scatterers are Circularly Shifted to Another Edge of the Range Profile Due to the Excessive Compensation Velocity.

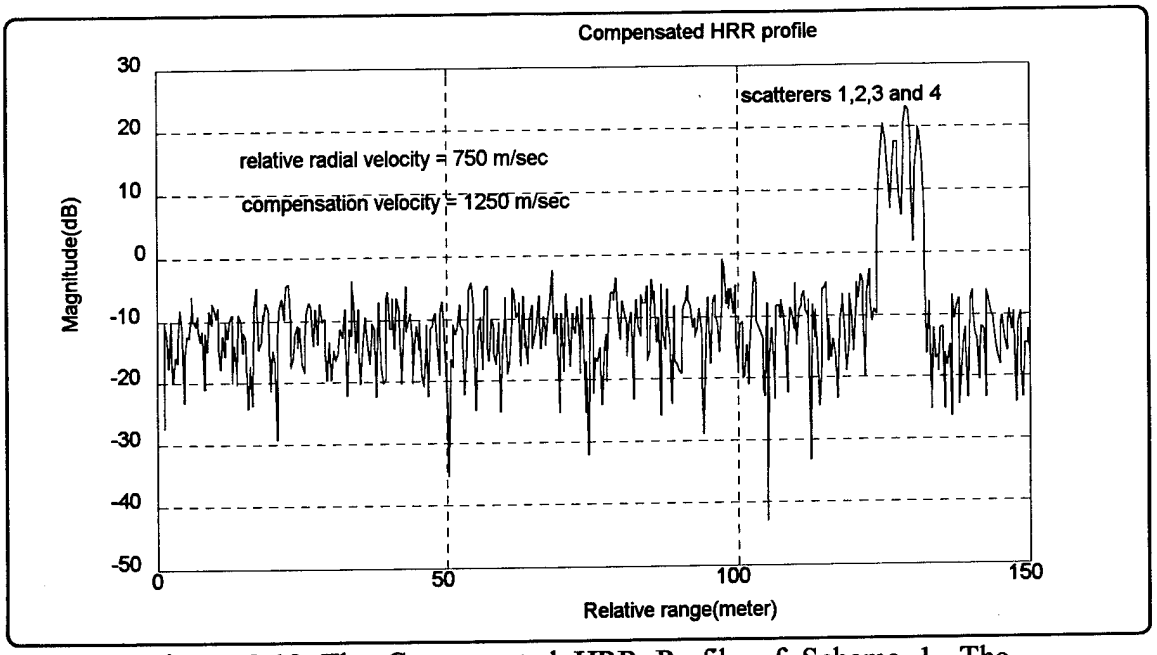

Figure 3.19 The Compensated HRR Profile of Scheme 1. The Clutter is Canceled. Compensation Velocity = 1250 m/sec. The Target Scatterers are Circularly Shifted to Another End of the Range Profile Due to the Excessive Compensation Velocity.

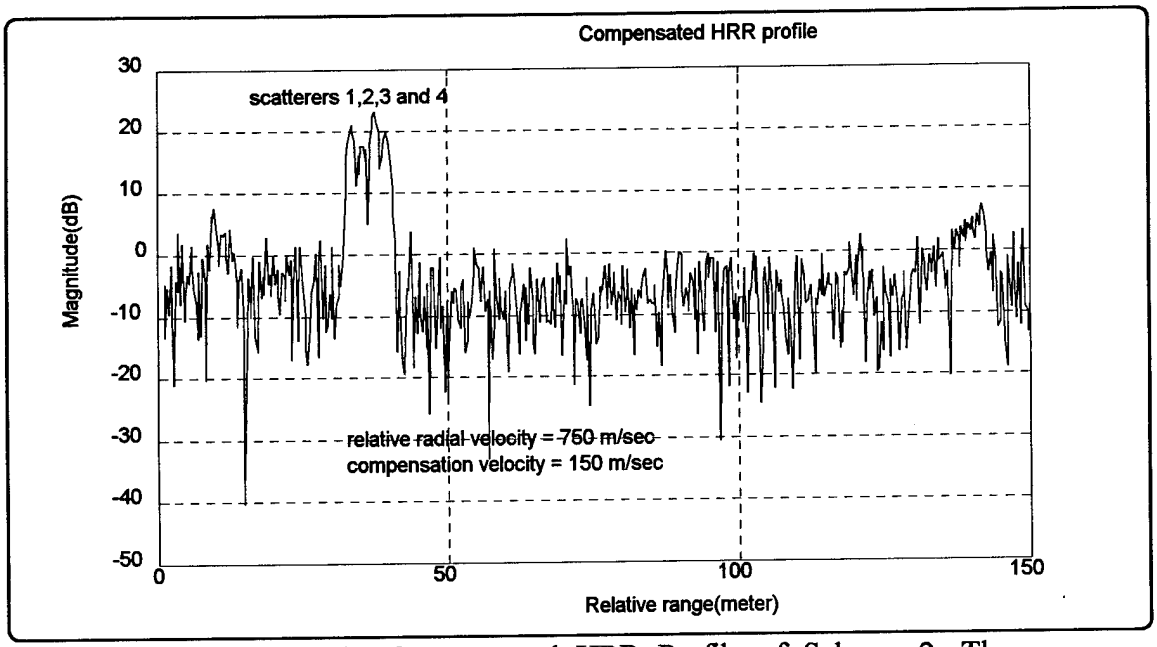

Figure 3.20 The Compensated HRR Profile of Scheme 2. The Clutter is Canceled. Compensation Velocity = 150 m/sec.

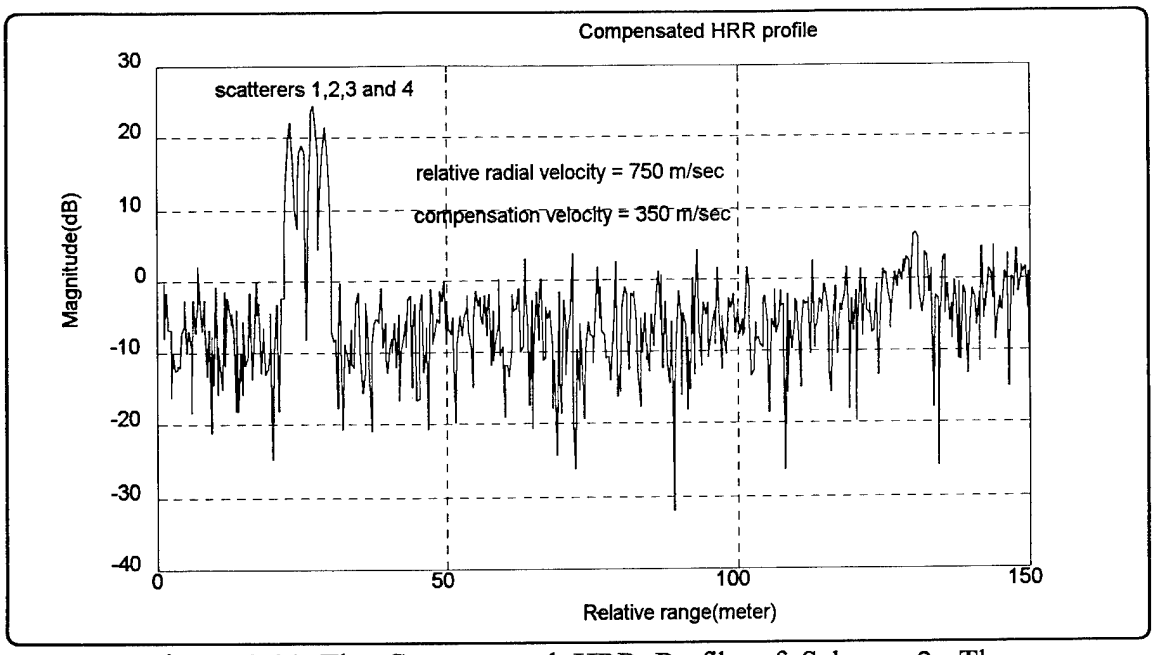

Figure 3.21 The Compensated HRR Profile of Scheme 2. The Clutter is Canceled. Compensation Velocity = 350 m/sec.

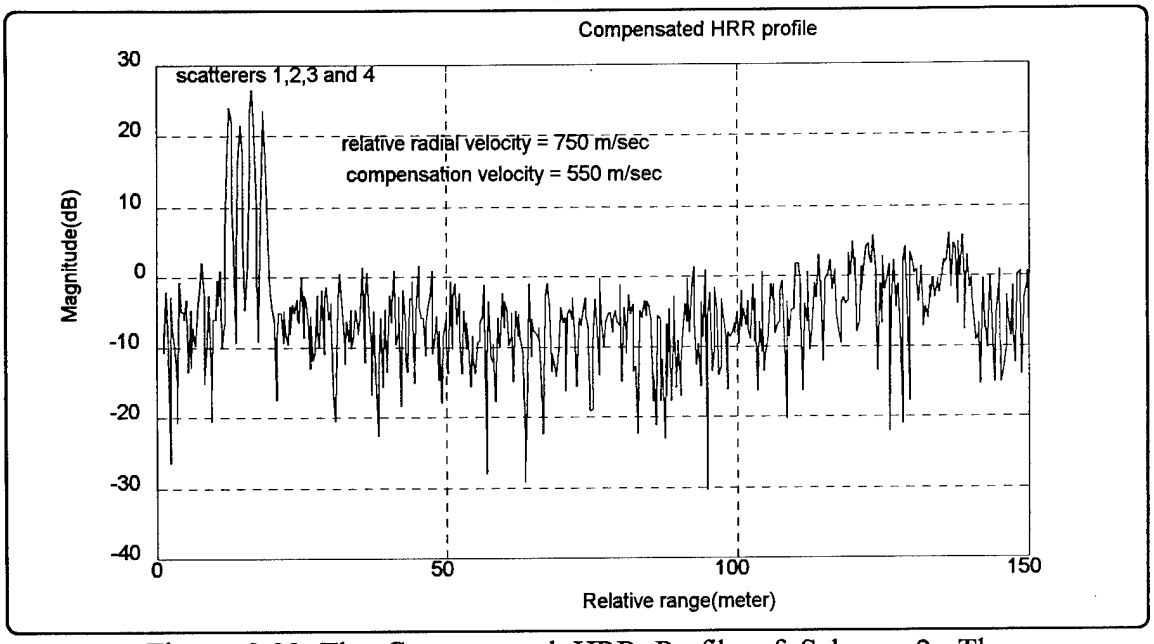

Figure 3.22 The Compensated HRR Profile of Scheme 2. The Clutter is Canceled. Compensation Velocity = 550 m/sec.

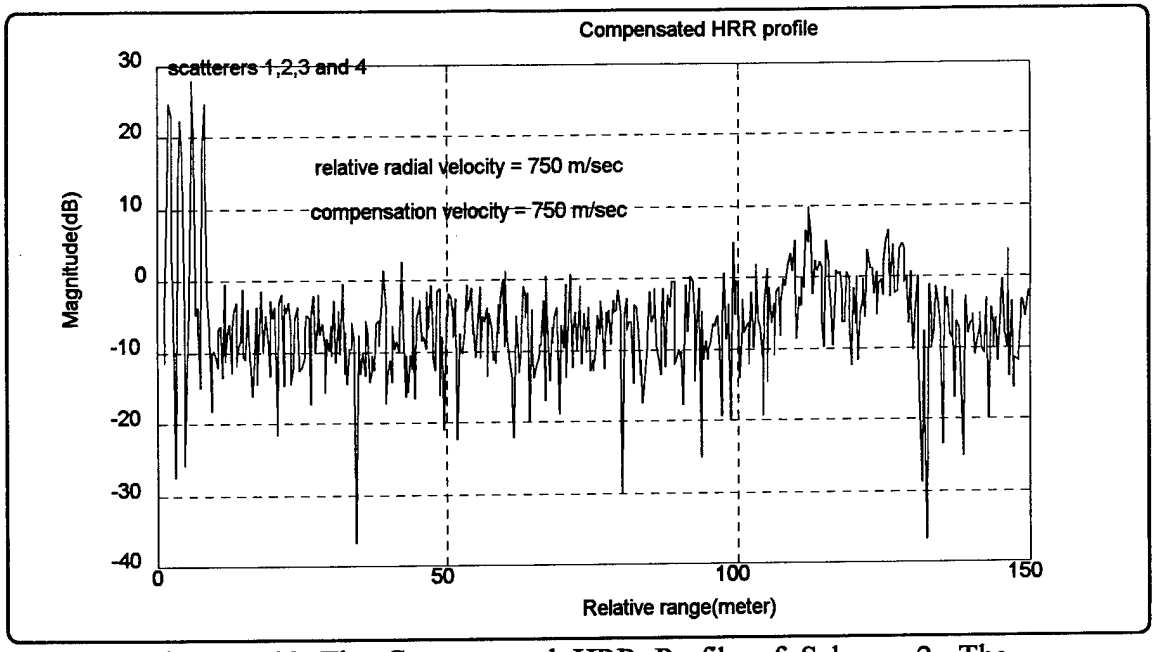

Figure 3.23 The Compensated HRR Profile of Scheme 2. The Clutter is Canceled. Compensation Velocity = 750 m/sec. This is a Correctly Velocity-Compensated HRR Profile.

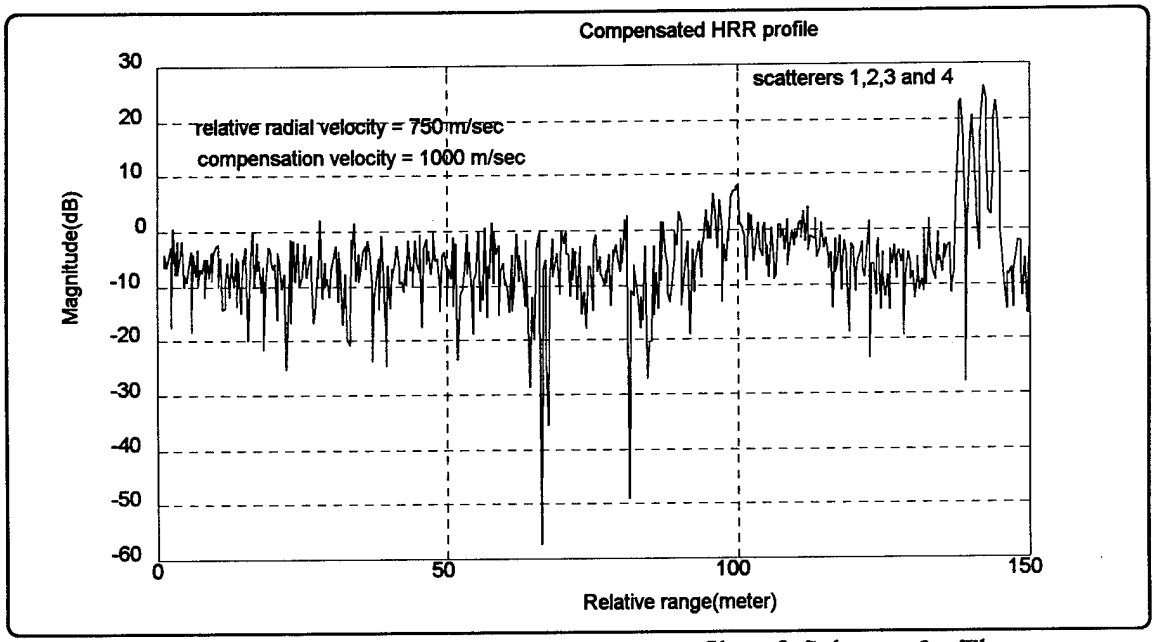

Figure 3.24 The Compensated HRR Profile of Scheme 2. The Clutter is Canceled. Compensation Velocity = 1000 m/sec. The Target Scatterers are Circularly Shifted to Another End of the HRR Profile Due to the Excessive Compensation Velocity.

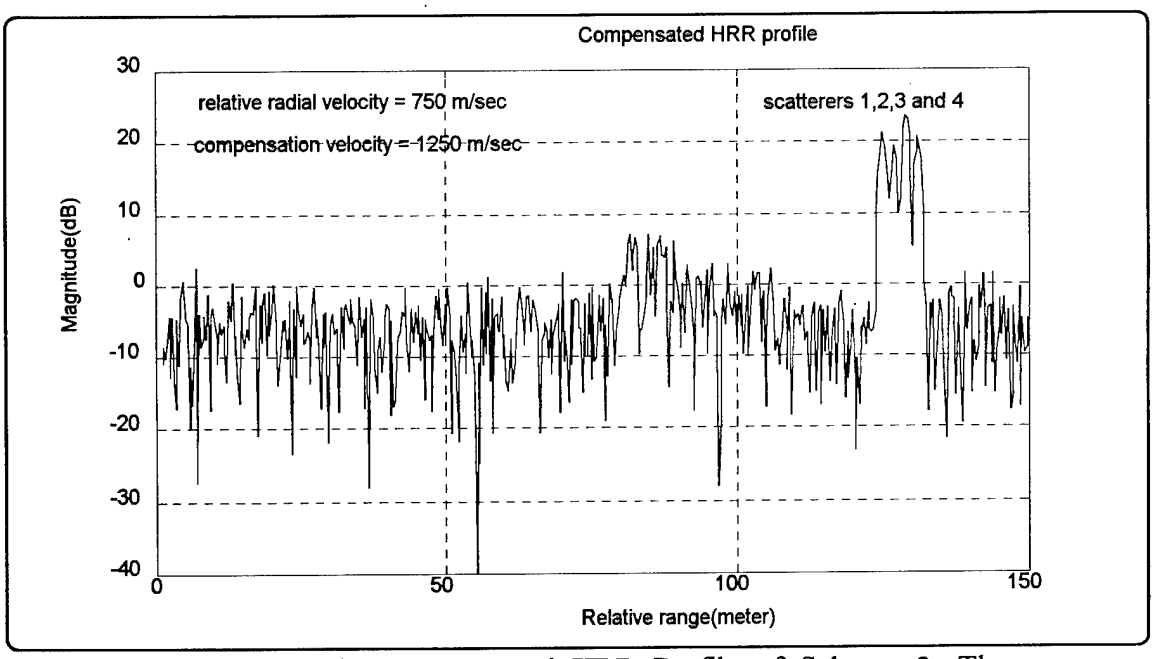

Figure 3.25 The Compensated HRR Profile of Scheme 2. The Clutter is Canceled. Compensation Velocity = 1250 m/sec. The Target Scatterers are Circularly Shifted to Another End of the HRR Profile Due to the Excessive Compensation Velocity.

3. Simulation of Scheme 3

In the simulation of scheme 3, the target approaches the radar platform at nose aspect at a velocity between Mach 2 and Mach 4 (approx. 660 m/sec to 1320 m/sec). The given initial compensation velocity is 660 m/sec, and the velocity step size, Δv, which is added in each compensation loop is 80 m/sec. The unknown target velocity, which is assumed between Mach 2 and Mach 4, is generated by using function "rand" in MATLAB. The simulation results are shown in Figure 3.26 through Figure 3.34.

As determined from the simulation results of compensation scheme 3, the compensated HRR profile of the eighth loop (Figure 3.34) has the best target resolution

and the largest *SNR*. Thus, it is estimated that the relative radial velocity is approximately equal to 1220 m/sec.

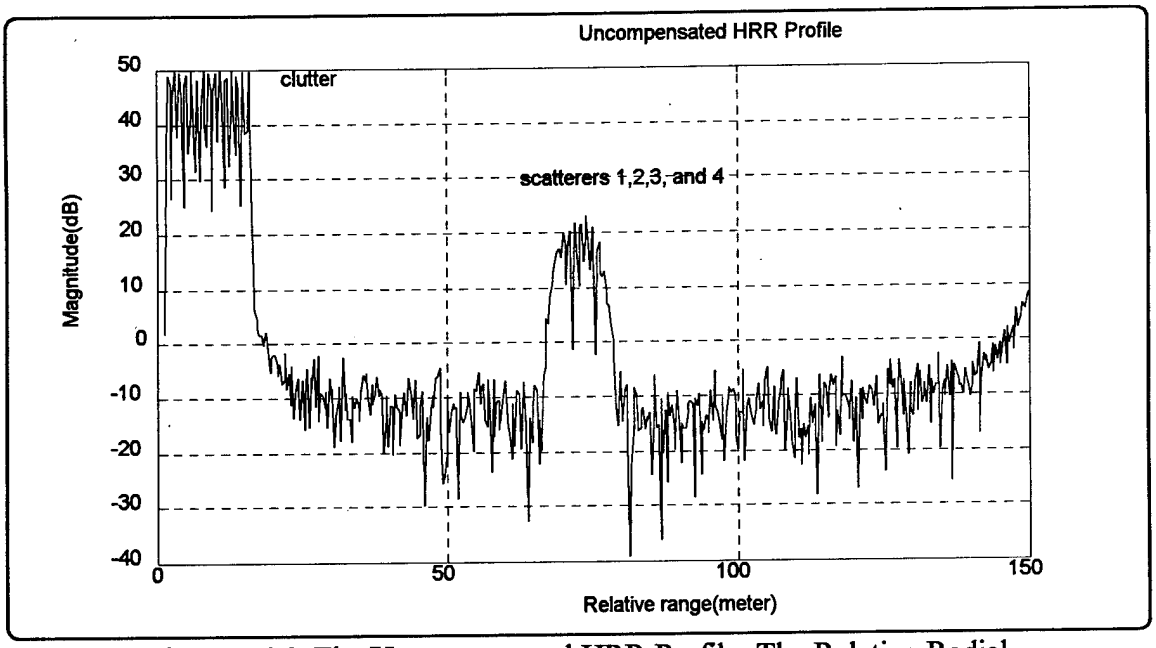

Figure 3.26 The Uncompensated HRR Profile. The Relative Radial Velocity is Unknown, But between Mach 2 and Mach 4.

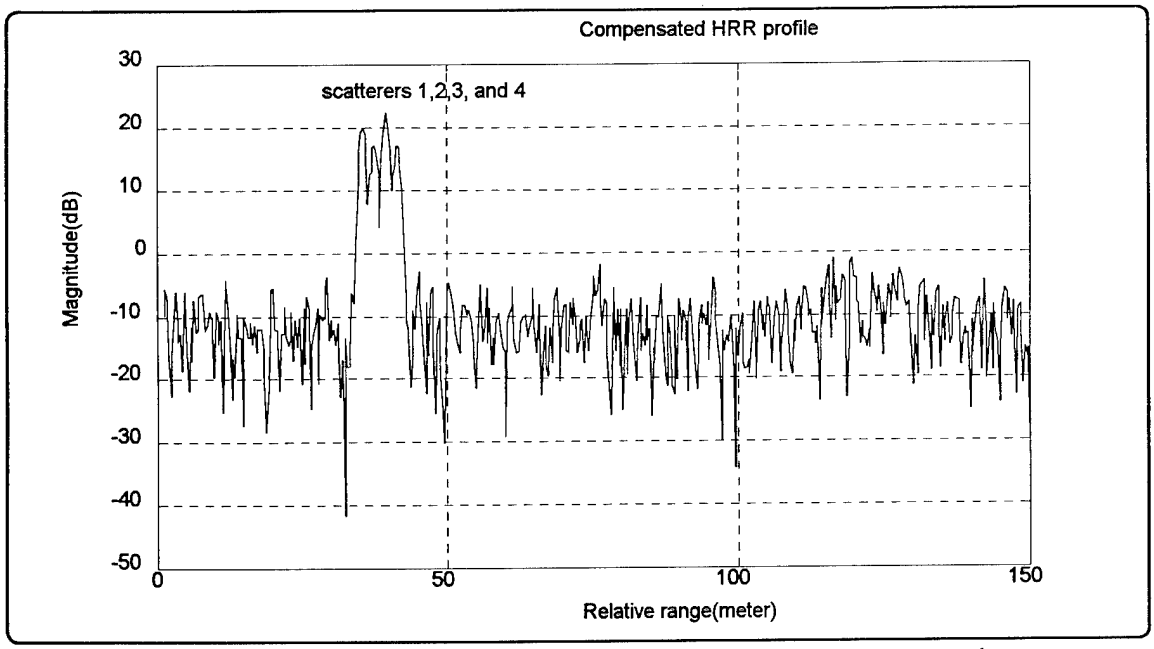

Figure 3.27 The Compensated HRR Profile of The First Loop. The Clutter is Canceled. Compensation Velocity = 660 m/sec.

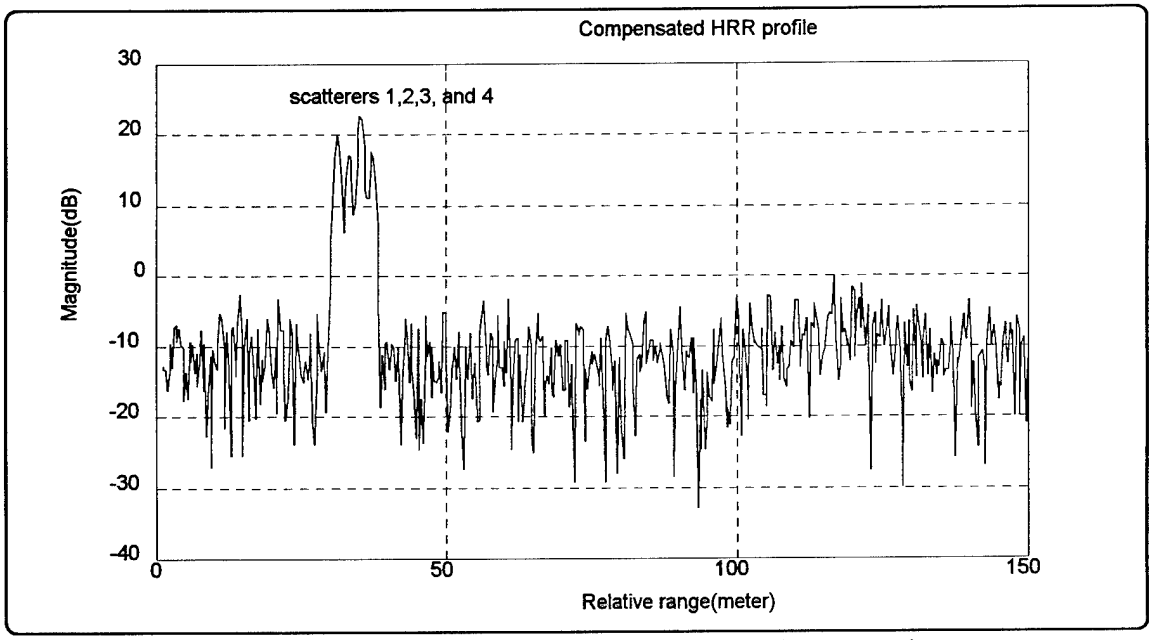

Figure 3.28 The Compensated HRR Profile of the Second Loop. The Clutter is Canceled. Compensation Velocity = 740 m/sec.

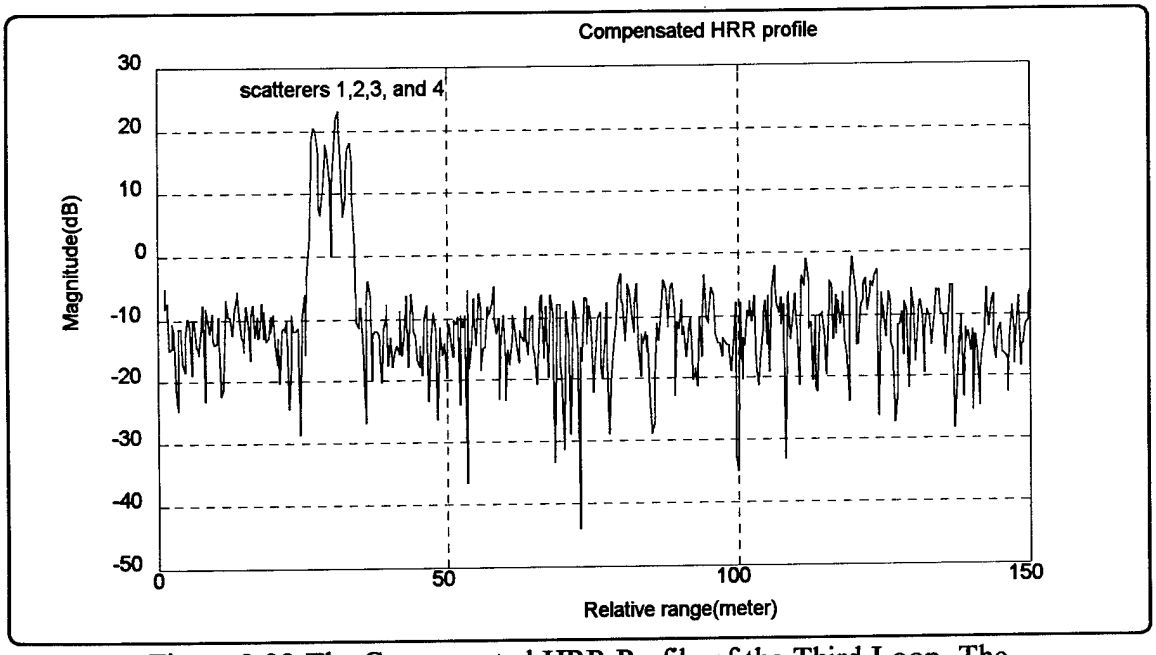

Figure 3.29 The Compensated HRR Profile of the Third Loop. The Clutter is Canceled. Compensation Velocity = 820 m/sec.

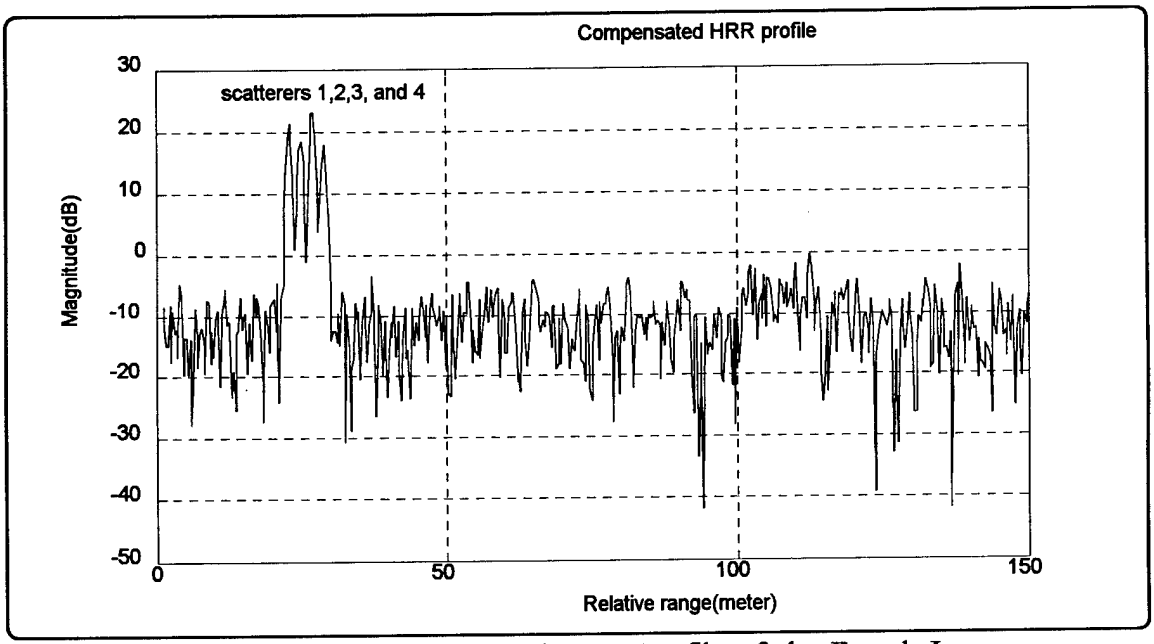

Figure 3.30 The Compensated HRR Profile of the Fourth Loop. The Clutter is Canceled. Compensation Velocity = 900 m/sec.

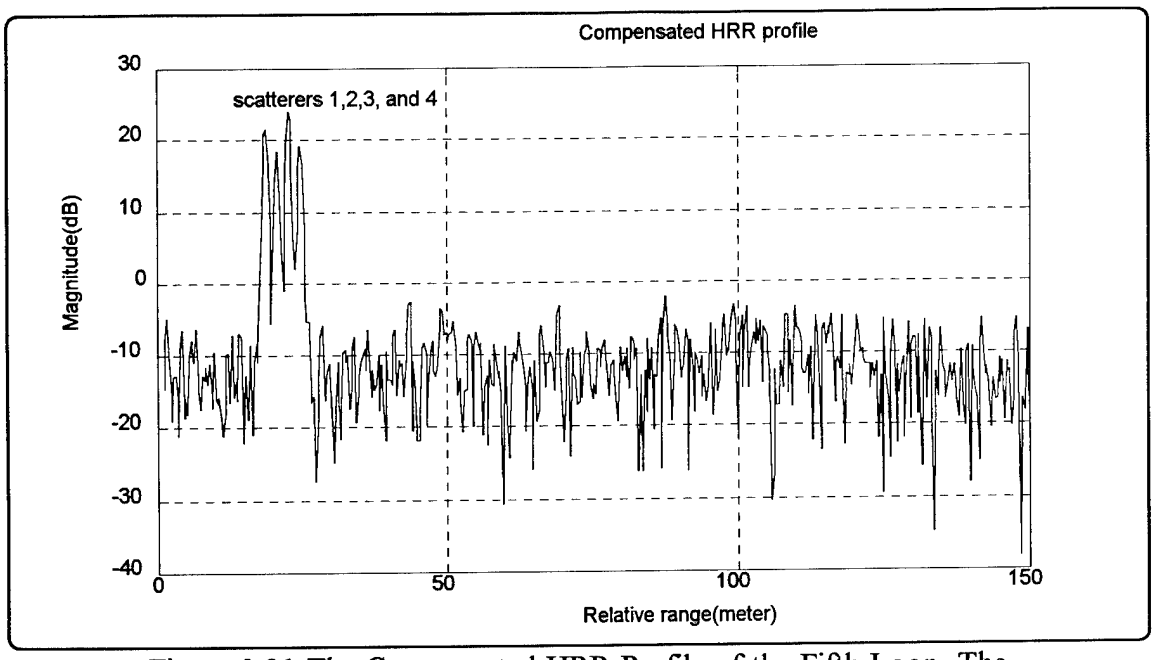

Figure 3.31 The Compensated HRR Profile of the Fifth Loop. The Clutter is Canceled. Compensation Velocity = 980 m/sec.

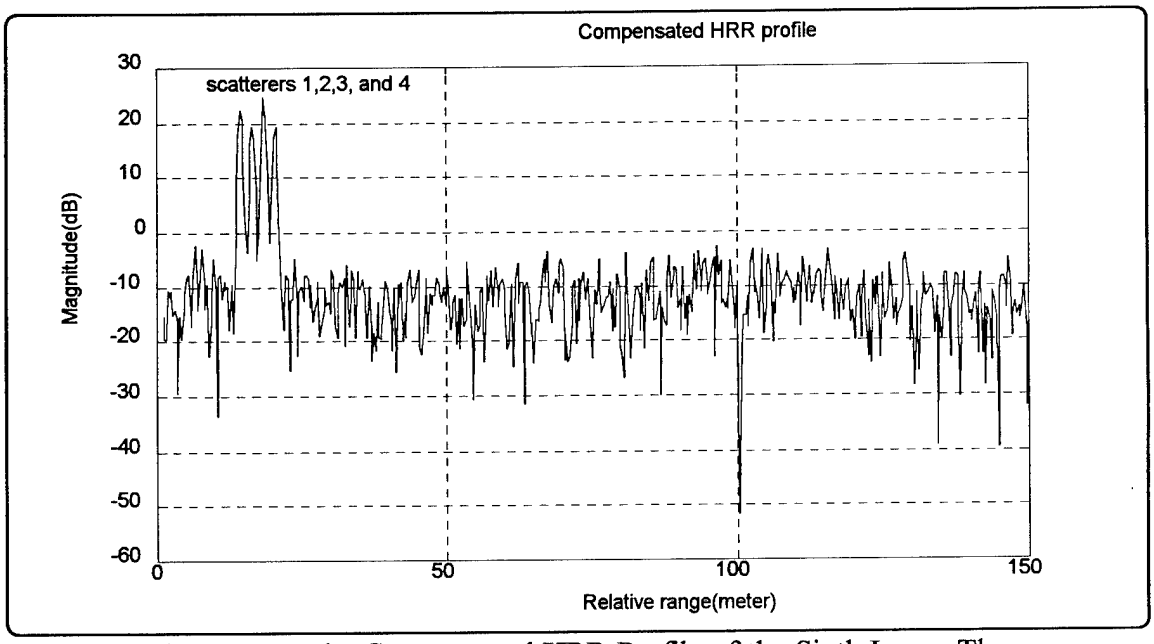

Figure 3.32 The Compensated HRR Profile of the Sixth Loop. The Clutter is Canceled. Compensation Velocity = 1060 m/sec.

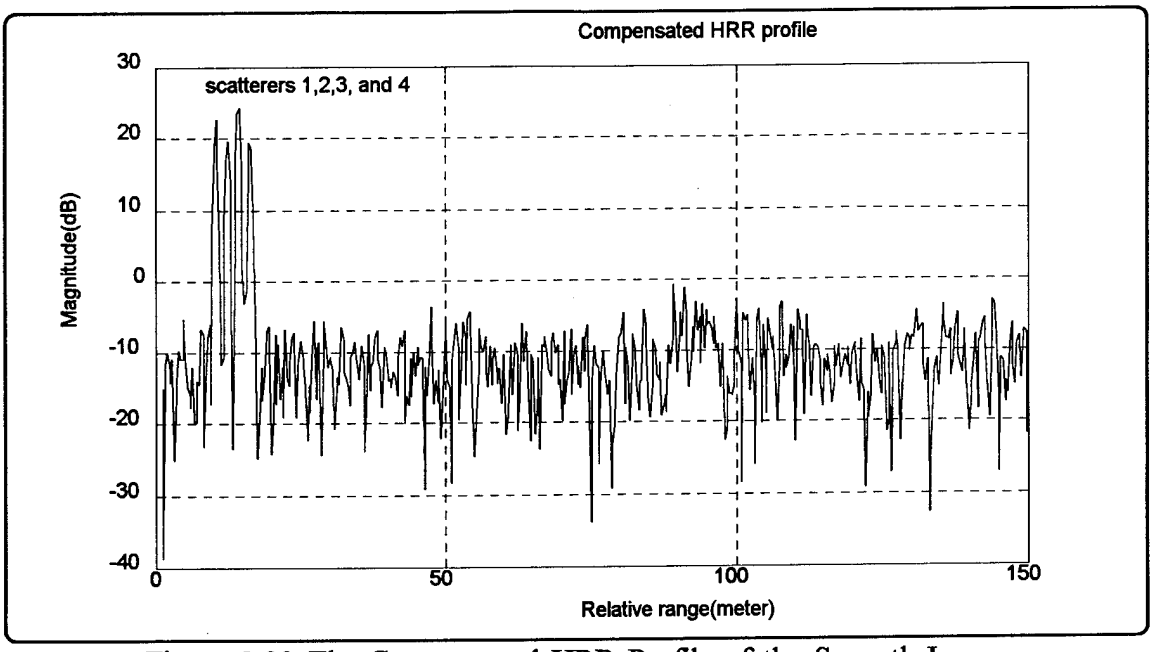

Figure 3.33 The Compensated HRR Profile of the Seventh Loop. The Clutter is Canceled. Compensation Velocity = 1140 m/sec.

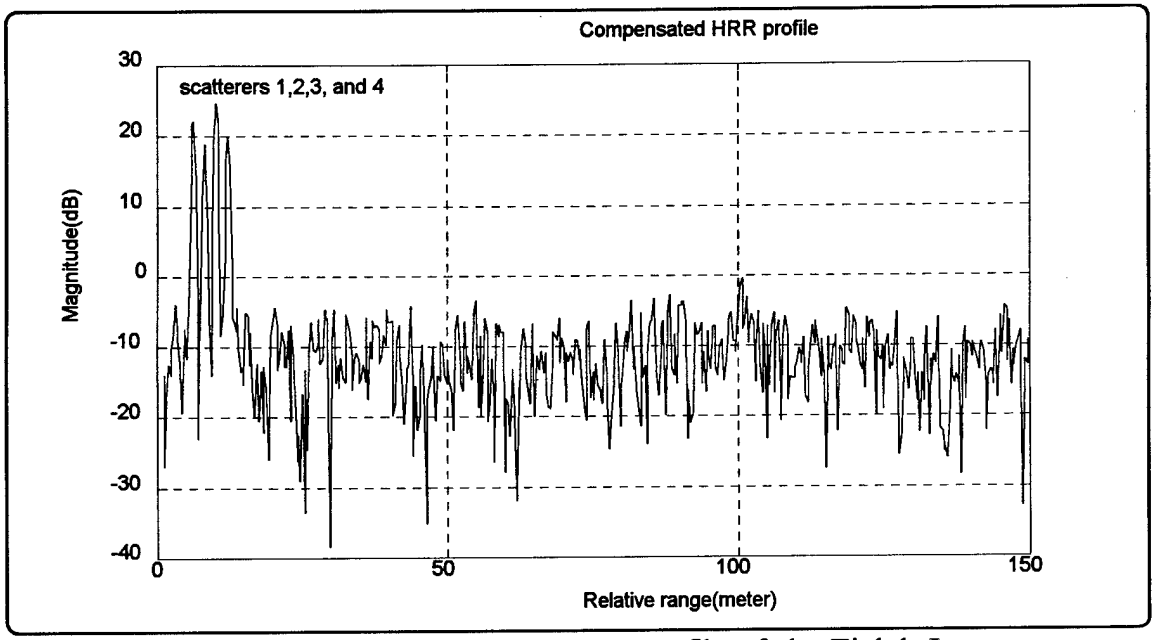

Figure 3.34 The Compensated HRR Profile of the Eighth Loop. The Clutter is Canceled. Compensated Velocity = 1220 m/sec.

(This page is intentionally left blank.)

IV. CONCLUSION

In the stepped-frequency radar, the high range resolution is achieved by performing the DFT on the received target signal. Nevertheless, this is optimum only when there is no relative radial velocity between the radar and the target. The nonlinear phase shifts induced by the relative motion cause a mismatch in the DFT process and result in a distorted range profile. Direct application of the velocity compensation factor to the received signal allows the compensation of the target signal; however, the clutter signal will disperse in the range profile due to the unnecessary compensation velocity. Thus, clutter cancellation has to be performed before velocity compensation in a velocity compensation scheme. In this thesis, three velocity compensation schemes have been presented to solve this problem.

In the design of the velocity compensation schemes, weighting functions are used to suppress range sidelobes in the compensated range profiles. It is found that in all three schemes, the use of a Hamming window prior to the first DFT has the maximum influence on sidelobe reduction. In addition, the second compensation scheme was originally expected to have higher computational speed than the first scheme due to fewer processing stages. However, because of the circular convolution of the compensation factor and the target signal, the complex multiplies used in the second scheme are much more than those required in the first scheme, resulting in significantly longer execution time. The first and the second schemes are theoretically equivalent, and both schemes generate very similar compensated HRR profiles for the same compensation velocity.

Nevertheless, since fewer Hamming windows are used in the second scheme, it is found that the compensated HRR profiles generated by the second scheme have higher range sidelobes and noise ripples. These phenomena can result in increased false alarms or reduced probability of target detection. From the viewpoint of fidelity and computational speed, the first scheme is considered better than the second scheme for implementation. The third scheme is based on the first scheme with the addition of a velocity compensation loop. In this case, the target velocity is unknown, but is assumed within a defined interval. In addition, it is observed that for the detection of moving targets using the stepped-frequency waveform, the use of a high PRF is appropriate for mapping high speed targets. The high PRF has the advantage of reducing the target dispersion even if accurate velocity compensation cannot be performed. However, a high PRF mode increases the system complexity.

Waveform design for the stepped-frequency radar is much more complex than that for the constant frequency radar. The selection of waveform parameters involves several tradeoffs that are not present in standard radars. A study to highlight these tradeoffs and to streamline the waveform design process should be conducted in the future.

APPENDIX A. SIGNAL MODELING

Target:

In the scenario of the simulation, there are 4 dominant scatterers on the target. The magnitudes of N return pulses from a specific scatterer on the target are assumed constant. Thus, the sampled scatterer signal of the phase detector for the nth pulse is given as

$$s_i(n) = A_i \exp(j\phi_n) \tag{A.1}$$

where

A_i = the constant magnitude of a specific scatterer for the nth return pulse

ϕ_n = the phase component of a scatterer for the nth pulse

n = 1, 2, 3, ..., N

i = index i is used to distinguished different scatterers on the target, i = 1, 2, 3, 4

The phase component of the sampled scatterer signal for the nth pulse is given by Eq.2.7 and Eq.2.9 as follows

$$\phi_n = 2\pi f_n \frac{2R_n}{c}$$

$$= 2\pi(f_0 + (n-1)\Delta f)\left(\frac{2(R_0 - (n-1)vT)}{c}\right)$$

$$= \frac{4\pi(f_0 + (n-1)\Delta f)(R_0 - (n-1)vT)}{c} \qquad \text{(A.2)}$$

where

Δf = the frequency step size from pulse to pulse

v = the relative radial velocity between the target and radar (- for opening velocity, + for closing velocity)

T = pulse repetition frequency

R_0 = the initial range when target is detected

c = the speed of light, 3×10^8 m/sec

Thus, a sampled scatterer signal is modeled as

$$s_i(n) = A_i \exp\left(j\frac{4\pi(f_0 + (n-1)\Delta f)(R_0 - (n-1)vT)}{c}\right) \qquad \text{(A.3)}$$

Clutter:

In the simulation, it is assumed that the stationary clutter distributes in an original range cell in which a moving target is located. Assume that there are 15 clutter sources, uniformly distributing in an original range cell (ΔR = 15 m) and the magnitudes of the return pulses from all 15 clutter source are constant. Similarly, the sampled clutter signal of each clutter source for the nth pulse can be modeled as

$$c_k(n) = C\exp\left(j\frac{4\pi(f_0 + (n-1)\Delta f)R_k}{c}\right) \tag{A.4}$$

where

C = the constant magnitude of the clutter signal

R_k = the range of each clutter source

k = index k is used to distinguished different clutter sources, $k = 1, 2, 3, ..., 15$.

Noise Source:

The thermal noise is modeled as white Gaussian noise with variance σ^2. The signal-to-noise ratio (*SNR*) is given by

$$SNR = \frac{A_i^2/2}{\sigma^2} = \frac{A_i^2}{2\sigma^2} \tag{A.5}$$

Thus, the constant magnitude of a scatterer signal can be written as

$$A_i = \sqrt{2\sigma^2(SNR)} \tag{A.6}$$

The clutter-to-noise ratio (*CNR*) is given by

$$CNR = \frac{C^2/2}{\sigma^2} = \frac{C^2}{2\sigma^2} \tag{A.7}$$

The constant magnitude of the clutter signal can also be written as

$$C = \sqrt{2\sigma^2(CNR)} \tag{A.8}$$

Overall Received Signal:

The overall received radar signal for the nth return pulse from an original range cell is modeled as

$$S(n) = \sum_{i=1}^{4} s_i\,(n) + \sum_{k=1}^{15} c_k\,(n) + noise(n) \tag{A.9}$$

where $noise(n)$ is a white Gaussian sequence.

APPENDIX B. SIMULATION PROGRAMS

```
function [ru, rstep]=scheme1(N,fstep,prf,r1,r2,r3,r4,v)
%%%%%%%%%%%%%%%%%%%%%%%%%%%%%%%%%%%%%%%%%%%%%%%%%%%%%%%%%%%%%%%%%%%%%%%%%%%%
%
% This program is a MATLAB function which computes the compensated HRR profile of
% 4-scatterer moving target in stationary clutter using scheme 1.This program include
% clutter cancellation followed by velocity compensation. The input data consists of
% following:
%       Number of pulses (N)
%       Frequency step size (fstep, Hz)
%       Pulse Repetition Frequency (prf, Hz)
%       Initial Scatter Ranges (r1,r2,r3,r4, meters)
%       Target Radial Velocity (v, m/sec)(-opening)(+closing)
% The following parameters can be changed within the function
%       Signal-to-Noise Ratio in (dB)  (SNR)
%       Clutter-to-Noise Ratio in (dB) (CNR)
%       Nominal Carrier Frequency (fo, Hz)
%       Velocity Matched for Compensation (co, m/sec)
% The outputs are Ru=c/2*fstep, and Rstep=Kc/2*n*fstep,
% which are the maximum unambiguous range and processed range bin size.
% The FFT size is equal to N.
%
%
%%%%%%%%%%%%%%%%%%%%%%%%%%%%%%%%%%%%%%%%%%%%%%%%%%%%%%%%%%%%%%%%%%%%%%%%%%%%

% Radar Parameters
fo=10*10^9;
n=0:N-1;
c=3*10^8;
f=fo+n*fstep;
K=1.33;
PRI=1/prf;
cnr=35; %dB
snr=13; %dB
a=10^(snr/10);
A3=sqrt(2*a*0.0002);
A1=sqrt(0.6)*A3;
A2=sqrt(0.3)*A3;
A4=sqrt(0.5)*A3;
b=10^(cnr/10);
C=sqrt(2*b*0.0002);
```

```
% Signal Modelings, Target, Clutter and Noise
s1=A1*exp(1j*(4*pi/c)*f.*(r1+n*v*PRI));
s2=A2*exp(1j*(4*pi/c)*f.*(r2+n*v*PRI));
s3=A3*exp(1j*(4*pi/c)*f.*(r3+n*v*PRI));
s4=A4*exp(1j*(4*pi/c)*f.*(r4+n*v*PRI));
c1=C*exp(1j*(4*pi/c)*1*f);
c2=C*exp(1j*(4*pi/c)*2*f);
c3=C*exp(1j*(4*pi/c)*3*f);
c4=C*exp(1j*(4*pi/c)*4*f);
c5=C*exp(1j*(4*pi/c)*5*f);
c6=C*exp(1j*(4*pi/c)*6*f);
c7=C*exp(1j*(4*pi/c)*7*f);
c8=C*exp(1j*(4*pi/c)*8*f);
c9=C*exp(1j*(4*pi/c)*9*f);
c10=C*exp(1j*(4*pi/c)*10*f);
c11=C*exp(1j*(4*pi/c)*11*f);
c12=C*exp(1j*(4*pi/c)*12*f);
c13=C*exp(1j*(4*pi/c)*13*f);
c14=C*exp(1j*(4*pi/c)*14*f);
c15=C*exp(1j*(4*pi/c)*15*f);
omega1=rand(size(n));
omega2=rand(size(n));
noise =sqrt(0.0002)*(omega1+1j*omega2);
s=s1+s2+s3+s4+(c1+c2+c3+c4+c5+c6+c7+c8+c9+c10+c11+c12+c13+c14+c15)+noise;
h=hamming(N)';
% Uncompensated HRR profile
s=s.*h;
S=fft(s);
ru=c/(2*fstep);
rstep=(K*c)/(2*N*fstep)
figure(1)
plot(n,20*log10(abs(S)))
grid
title('Uncompensated HRR profile ')
xlabel('Relative range(meter)')
ylabel('Magnitude(dB)')
figure(2)
t=linspace(1,ru,512);
plot(t,20*log10(abs(S)))
grid
title('Uncompensated HRR profile ')
xlabel('Relative range(meter)')
ylabel('Magnitude(dB)')
```

```
% Clutter Cancellation
bu=input('Enter high bin number for clutter')
co=input('Enter compensation velocity for target ')
vc=exp(-1j*(4*pi*PRI/c)*(co)*f.*n);
ss1=[zeros(size(1:bu)) ones(size(1:N-bu))].*S;
% Velocity Compensation
SS1=ifft(ss1).*vc;
% Second Weighting
SS1=SS1.*h;
% Compensated HRR profile
FSS=fft(SS1);
figure(3)
plot(t,20*log10(abs(FSS)))
grid
title('Compensated HRR profile')
xlabel('Relative range(meter)')
ylabel('Magnitude(dB)')
gtext('scatterers 1,2,3 and 4')
```

```
function [ru, rstep]=scheme2(N,fstep,prf,r1,r2,r3,r4,v)
%%%%%%%%%%%%%%%%%%%%%%%%%%%%%%%%%%%%%%%%%%%%%%%%%%%%%%%%%%%%%%%%%%%%%%%%%%%%
%
% This program is a MATLAB function which computes the compensated HRR profile of
% 4-scatterer moving target in stationary clutter using scheme 2.This program include
% clutter cancellation followed by velocity compensation. The input data consists of
% following:
%       Number of pulses (N)
%       Frequency step size (fstep)
%       Pulse Repetition Frequency (prf)
%       Initial Scatter Ranges (r1,r2,r3,r4)
%       Target Radial Velocity (v)(-opening)(+closing)
% The following parameters can be changed within the function
%       Signal-to-Noise Ratio in (dB) (SNR)
%       Clutter-to-Noise Ratio in (dB) (CNR)
%       Nominal Carrier Frequency (fo)
%       Velocity Matched for Compensation (co)
% The outputs are Ru=c/2*fstep, and Rstep=Kc/2*n*fstep,
% which are the maximum unambiguous range and processed range bin size.
%The FFT size is equal to N.
%
%
%%%%%%%%%%%%%%%%%%%%%%%%%%%%%%%%%%%%%%%%%%%%%%%%%%%%%%%%%%%%%%%%%%%%%%%%%%%%

% Radar Parameters
fo=10*10^9;
n=0:N-1;
c=3*10^8;
K=1.33;
PRI=1/prf;
cnr=35;%dB
snr=13;%dB
a=10^(snr/10);
A3=sqrt(2*a*0.0002);
A1=sqrt(0.6)*A3;
A2=sqrt(0.3)*A3;
A4=sqrt(0.5)*A3;
b=10^(cnr/10);
C=sqrt(2*b*0.0002);
% Signal Modelings: Targets, Clutters & Noise
f=fo+n*fstep;
s1=A1*exp(1j*(4*pi/c)*f.*(r1+n*v*PRI));
s2=A2*exp(1j*(4*pi/c)*f.*(r2+n*v*PRI));
```

```
s3=A3*exp(1j*(4*pi/c)*f.*(r3+n*v*PRI));
s4=A4*exp(1j*(4*pi/c)*f.*(r4+n*v*PRI));
c1=C*exp(1j*(4*pi/c)*1*f);
c2=C*exp(1j*(4*pi/c)*2*f);
c3=C*exp(1j*(4*pi/c)*3*f);
c4=C*exp(1j*(4*pi/c)*4*f);
c5=C*exp(1j*(4*pi/c)*5*f);
c6=C*exp(1j*(4*pi/c)*6*f);
c7=C*exp(1j*(4*pi/c)*7*f);
c8=C*exp(1j*(4*pi/c)*8*f);
c9=C*exp(1j*(4*pi/c)*9*f);
c10=C*exp(1j*(4*pi/c)*10*f);
c11=C*exp(1j*(4*pi/c)*11*f);
c12=C*exp(1j*(4*pi/c)*12*f);
c13=C*exp(1j*(4*pi/c)*13*f);
c14=C*exp(1j*(4*pi/c)*14*f);
c15=C*exp(1j*(4*pi/c)*15*f);
omega1=rand(size(n));
omega2=rand(size(n));
noise =sqrt(0.0002)*(omega1+1j*omega2);
s=s1+s2+s3+s4+(c1+c2+c3+c4+c5+c6+c7+c8+c9+c10+c11+c12+c13+c14+c15)+noise;
h=hamming(N)';
%  Uncompensated HRR profile
s=s.*h;
S=fft(s);
ru=c/(2*fstep);
rstep=(K*c)/(2*N*fstep)
figure(1)
t=linspace(1,ru,N);
plot(t,20*log10(abs(S)))
grid
title('Uncompensated HRR Profile')
xlabel('Relative range(meter)')
ylabel('Magnitude(dB)')
figure(2)
plot(t,20*log10(abs(S)))
grid
title('Uncompensated HRR Profile')
xlabel('Relative range(meter)')
ylabel('Magnitude(dB)')
% Clutter Cancellation
bu=input('Enter high bin number for clutter')
co=input('Enter compensation velocity for target ')
```

```
vc=exp(-1j*(4*pi*PRI/c)*co*f.*n);
ss1=[zeros(size(1:bu)) ones(size(1:N-bu))].*S;
% DFT of Velocity Compensation Factor
vc=(1/N)*fft(vc);
%  Velocity Compensation
SS1=circonv(ss1,vc);
%  Compensated HRR profile
figure(3)
plot(t,20*log10(abs(SS1)))
grid
title('Compensated HRR profile')
xlabel('Relative range(meter)')
ylabel('Magnitude(dB)')
gtext('scatterers 1,2,3 and 4')
```

```
function [value]=circonv(x1,x2)
%%%%%%%%%%%%%%%%%%%%%%%%%%%%%%%%%%%%%%%%%%%%%%%%
%
% This MATLAB function is to calculate cicular convolution via direct approach. Both x1
% and x2 are sequences of length N. The resulting sequence of cicular
% convolution has also the same length N.
%
%
 %%%%%%%%%%%%%%%%%%%%%%%%%%%%%%%%%%%%%%%%%%%%%%%%

k=2:length(x2);
A(1,1)=x2(1);
A(1,k)=x2(length(x2)-(k-2));
value(1)=sum(x1.*A(1,:));
for i=2:length(x2);
for k=2:length(x2);
   A(i,1)=A(i-1,length(x2));
   A(i,k)=A(i-1,k-1);
end
value(i)=sum(x1.*A(i,:));
end
```

```
function [ru, rstep]=scheme3(N,fstep,prf,r1,r2,r3,r4)
%%%%%%%%%%%%%%%%%%%%%%%%%%%%%%%%%%%%%%%%%%%%%%%%%%%%%%%%%%%%%%%%%%%%%%%%%
%
% This program is a MATLAB function which computes the compensated HRR profile of
% 4-scatterer moving target in stationary clutter using scheme 3.This program include
% clutter cancellation followed by velocity compensation. The input data consists of
% following:
%       Number of pulses (N)
%       Frequency step size (fstep)
%       Pulse Repetition Frequency (prf)
%       Initial Scatter Ranges (r1,r2,r3,r4)
% The following parameters can be changed within the function
%       Signal-to-Noise Ratio in (dB) (SNR)
%       Clutter-to-Noise Ratio in (dB) (CNR)
%       Nominal Carrier Frequency (fo)
%       Initial Compensation Velocity (v)(-opening)(+closing)
%       Velocity Matched for Compensation (co)
% The outputs are Ru=c/2*fstep, and Rstep=Kc/2*n*fstep,
% which are the maximum unambiguous range and processed range bin size.
% The FFT size is equal to N.
%
%
%%%%%%%%%%%%%%%%%%%%%%%%%%%%%%%%%%%%%%%%%%%%%%%%%%%%%%%%%%%%%%%%%%%%%%%%%

% Radar Parameters
v=-(660+660*rand(1));
fo=10*10^9;
n=0:N-1;
c=3*10^8;
K=1.33;
PRI=1/prf;
cnr=35;
snr=13;
a=10^(snr/10);
A3=sqrt(2*a*0.0002);
A1=sqrt(0.6)*A3;
A2=sqrt(0.3)*A3;
A4=sqrt(0.5)*A3;
b=10^(cnr/10);
C=sqrt(2*b*0.0002);
% Signal Modelings: Targets, Clutter & Noise
f=fo+n*fstep;
s1=A1*exp(1j*(4*pi/c)*f.*(r1-n*v*PRI));
```

```
s2=A2*exp(1j*(4*pi/c)*f.*(r2-n*v*PRI));
s3=A3*exp(1j*(4*pi/c)*f.*(r3-n*v*PRI));
s4=A2*exp(1j*(4*pi/c)*f.*(r4-n*v*PRI));
c1=C*exp(1j*(4*pi/c)*1*f);
c2=C*exp(1j*(4*pi/c)*2*f);
c3=C*exp(1j*(4*pi/c)*3*f);
c4=C*exp(1j*(4*pi/c)*4*f);
c5=C*exp(1j*(4*pi/c)*5*f);
c6=C*exp(1j*(4*pi/c)*6*f);
c7=C*exp(1j*(4*pi/c)*7*f);
c8=C*exp(1j*(4*pi/c)*8*f);
c9=C*exp(1j*(4*pi/c)*9*f);
c10=C*exp(1j*(4*pi/c)*10*f);
c11=C*exp(1j*(4*pi/c)*11*f);
c12=C*exp(1j*(4*pi/c)*12*f);
c13=C*exp(1j*(4*pi/c)*13*f);
c14=C*exp(1j*(4*pi/c)*14*f);
c15=C*exp(1j*(4*pi/c)*15*f);
omega1=rand(size(n));
omega2=rand(size(n));
noise =sqrt(0.0002)*(omega1+1j*omega2);
s=s1+s2+s3+s4+(c1+c2+c3+c4+c5+c6+c7+c8+c9+c10+c11+c12+c13+c14+c15)+noise;
h=hamming(N)';
% Uncompensated HRR profile
s=s.*h;
S=fft(s);
mag=abs(S);
ru=c/(2*fstep);
rstep=(K*c)/(2*N*fstep)
figure(1)
plot(n,20*log10(mag))
grid
title('Uncompensated HRR Profile')
xlabel('Relative range(meter)')
ylabel('Magnitude(dB)')
figure(2)
t=linspace(1,ru,512);
plot(t,20*log10(mag))
grid
title('Uncompensated HRR Profile')
xlabel('Relative range(meter)')
ylabel('Magnitude(dB)')
% Clutter Cancellation
```

```
bu=input('Enter high bin number for clutter')
co= -660;
M=1:8;
cco=co-(M-1)*80;
for P=1:8
vc=exp(1j*(4*pi*PRI/c)*cco(P)*f.*n);
ss1=[zeros(size(1:bu)) ones(size(1:N-bu))].*S;
% Velocity Compensation
SS1=ifft(ss1).*vc;
% Second Weighting
SS1=SS1.*h;
% Compensated HRR profile
FSS=fft(SS1);
figure(P+2)
plot(t,20*log10(abs(FSS)))
grid
title('Compensated HRR profile')
xlabel('Relative range(meter)')
ylabel('Magnitude(dB)')
end
```

LIST OF REFERENCES

1. Donald R. Wehner, *High Resolution Radar*, Artech House Inc., Boston, MA, 1985.

2. James A. Scheer, and James L. Kurtz, *Coherence Radar Performance Estimation*, Artech House Inc., Boston, MA, 1983.

3. Lincoln Laboratory, Project Report TT-54, *Generation of High Resolution Radar Range Profiles and Auto-Correlation Functions Using Stepped-Frequency Pulse Trains*, by T.H.Einstein, October, 1984.

4. Robert D. Strum and Donald E. Kirk, *First Principles of Discrete Systems and Digital Signal Processing*, Addison Wesley Publishing Company, MA, 1988.

5. The Math Works, Inc., *The Student Edition of Matlab*, Prentice-Hall, Inc., Englewood Cliffs, NJ, 1992.

6. Fred E. Nathanson, *Radar Design Principles*, Second Edition, McGraw-Hill, Inc., New York, NY, 1991.

7. George W. Stimson, *Introduction to Airborne Radar*, Hughes Aircraft Company, El Segundo, CA, 1983.

(This page is intentionally left blank.)

INITIAL DISTRIBUTION LIST

1. Defense Technical Information Center — 2
   8725 John J. Kingman Rd., STE 0944
   Ft. Belvoir, VA 22060-6218

2. Library Code 013 — 2
   Naval Postgraduate School
   Monterey, CA 93943-5101

3. Chairman, Code EC — 1
   Department of Electrical and Computer Engineering
   Naval Postgraduate School
   Monterey, CA 93943-5121

4. Professor G.S. Gill, Code EC/Gl — 4
   Department of Electrical and Computer Engineering
   Naval Postgraduate School
   Monterey, CA 93943-5121

5. Professor David C. Jenn, Code EC/Jn — 1
   Department of Electrical and Computer Engineering
   Naval Postgraduate School
   Monterey, CA 93943-5121

6. Maj. Ma Yu-Bin — 2
   War Game Center, Armed Forces University
   P.O. Box 90040-16 Ta-Chi,
   Taipei, Taiwan 104

7. Dr. Thomas E. Tice — 1
   Code 755
   NCCOSC, NRaD
   San Diego, CA 92152-5000

8. Dr. W. Miceli 1
Office of Naval Research
Attn: ONR 313
Ballston Tower 1
800 N. Quincy St.
Arlington, VA. 22203